学 位 論 文

Studies on molecular mechanisms underlying 5-ALA mediated fluorescence-guided surgery and the prognostic significance of CD44 in grade II/III gliomas

（グレードII/III神経膠腫における5-ALAを利用した蛍光誘導手術の分子機構とCD44の予後への重要性に関する研究）

2020 年 3 月

北　海　道　大　学

コウ　スウケン

Hou Chongxian

学 位 論 文

Studies on molecular mechanisms underlying 5-ALA mediated fluorescence-guided surgery and the prognostic significance of CD44 in grade II/III gliomas

（グレードII/III神経膠腫における5-ALAを利用した蛍光誘導手術の分子機構とCD44の予後への重要性に関する研究）

2020 年 3 月

北　海　道　大　学

コウ　スウケン

Hou Chongxian

Tables of Contents

List of Publications and Presentations

List of Publications

1. **Hou C**, Yamaguchi S, Ishi Y, Terasaka S, Kobayashi H, Motegi H, Hatanaka KC, Houkin K. Identification of PEPT2 as an important candidate molecule in 5-ALA-mediated fluorescence-guided surgery in WHO grade II/III gliomas. J Neurooncol Jun;143(2):197-206. 2019

2. **Hou C**, Ishi Y, Motegi H, Okamoto M, Ou Y, Chen J, Yamaguchi S. Overexpression of CD44 is associated with a poor prognosis in grade II/III gliomas. J Neurooncol Nov;145(2):201-210. 2019

3. Wang P, **Hou C (co-first author)**, Li Y, Zhou D. Wireless Phone Use and Risk of Adult Glioma: Evidence from a Meta-Analysis. World neurosurgery 115: e629-e636 2018

4. Chen J, **Hou C (co-first author)**, Zheng Z, Lin H, Lv G, Zhou D. Identification of Secreted Phosphoprotein 1 (SPP1) as a Prognostic Factor in Lower-Grade Gliomas. World neurosurgery 130: e775-e785 2019

List of Presentations

1. **Hou C**, Yamaguchi S, Ishi Y, Terasaka S, Kobayashi H, Motegi H, Houkin K. The 19th Annual Meeting of the Japan Society of Molecular Neurosurgery, July 24-25, 2018, Osaka, Japan.

Summary

Background and purpose:

Glioma is the most frequent primary malignant brain tumor. Surgery, combined with chemotherapy and radiotherapy, is the standard treatment; however, glioma remains incurable due to its high recurrence rate and invasiveness. Thus, studies on new therapeutic approaches and targets for gliomas are of great importance. The present study mainly focused on two topics for glioma, The first topic is the study on key molecules in 5-aminolevulinic acid (5-ALA) mediated fluorescence-guided surgery (FGS) in grade II/III gliomas and the second topic is the study on the prognostic significance of CD44 in grade II/III gliomas.

Patients with glioma can benefit from the maximum safest resection. However, surgeons often have difficulty distinguishing tumor tissue from normal tissue and in recognizing infiltrating glioma cells in normal tissues adjacent to tumor tissue intraoperatively. In addition, >90% of recurrent gliomas occur within 2–3 cm of the borders of the original tumor lesion. 5-ALA mediated FGS appears to be a promising treatment for glioma. However, 5-ALA-mediated fluorescence cannot always be detected in the World Health Organization grade II/III gliomas. It was hypothesized that gene expression patterns in the Protoporphyrin IX (PpIX) synthesis pathway may be associated with the intraoperative fluorescence status of grade II/III gliomas, and the first part of this study attempted to identify the key molecule of 5-ALA-mediated fluorescence.

CD44 is a major cell surface receptor for hyaluronan (HA) and many other extracellular matrix components, and is implicated in cell adhesion, cell migration, and signaling. Overexpression of CD44 has been detected in many types of tumor tissues. Moreover, CD44 is recognized as a cancer stem cell marker for many cancers. However, the prognostic value of CD44 for glioma patients has not yet been clarified. We tried to explore the impact of CD44 expression on grade II/III glioma patients.

(Studies on key molecules in 5-ALA mediated fluorescence-guided surgery in grade II/III gliomas)

Methods and materials:

The present study first attempted to identify candidate genes with an effect on 5-ALA-mediated PpIX fluorescence intensity. The mRNA expression levels of genes (*ALAD, ALAS1, ABCG2, ABCB6, CPOX, FECH, HO-1, PEPT2* and *UROS*) in the PpIX synthesis pathway were compared among normal brain tissues, fluorescence-negative grade II/III gliomas, and fluorescence-positive grade II/III gliomas. The most likely candidate gene was selected and confirmed by protein expression analysis. To further investigate the exact function of the target gene, the mRNA and protein expression of the target gene was inhibited in a grade III glioma cell line and the PpIX fluorescence spectrum was detected.

Results and discussion:

The mRNA expression levels of *ALAD*, *ABCG2*, *ABCB6*, *CPOX*, *HO-1*, *PEPT2*, and *UROS* were significantly higher in the fluorescence-positive grade II/III gliomas than the fluorescence-negative grade II/III gliomas. Among the above candidate genes, the present study focused on PEPT2 because it is an upstream molecule in the PpIX synthesis pathway and PEPT2 plays an important role in the selective transportation of peptides, amino acids, and drugs of the cells in the central nervous system. The protein expression of PEPT2 was also significantly higher in the fluorescence-positive gliomas, which was confirmed by western blot analysis and immunofluorescence analysis. The siRNA-mediated downregulation of the mRNA and protein expression of PEPT2 led to decreased PpIX fluorescence intensity, as confirmed by fluorescence spectrum analysis. Through down-regulating the expression of PEPT2, the fluorescence intensity may be managed by neurosurgeons in the future.

(Studies on the prognostic significance of CD44 in grade II/III gliomas)

Methods and materials:

To assess the RNA expression levels of *CD44* in glioma tissues and normal brain tissues, meta-analyses were conducted in the online Oncomine database. Based on the Oncomine

database, *CD44* has significantly high expression in glioma tissues as compared with normal tissues. Then, the mRNA expression levels of *CD44*, *CD44s*, and *CD44v2–v10* in 112 grade II/III glioma patients in Hokkaido University Hospital (HUH) were detected by qPCR. The RNA-seq data and clinical data of grade II/III glioma patients were obtained from The Cancer Genome Atlas (TCGA) and the Chinese Glioma Genome Atlas (CGGA) databases. The Kaplan-Meier survival curve analysis was performed to explore the association between CD44 gene expression and overall survival of glioma patients. Then we used univariate and multivariate Cox regression analyses to evaluate the utility of *CD44* expression as an independent prognostic factor. Gene Set Enrichment Analysis (GSEA) was performed to explore the function of *CD44* and its related signaling pathways base on the TCGA database.

Results and discussion:

In the study on the prognostic significance of CD44, based on the Oncomine database, *CD44* has significantly high expression in glioma tissues as compared with normal tissues. Compared with mRNA expression level of CD44s, the mRNA expression levels of *CD44v2*, *CD44v3*, *CD44v4*, *CD44v5*, *CD44v6*, *CD44v7*, *CD44v8*, *CD44v9*, and *CD44v10* were much lower. Besides, tumor specimens which belonged to *CD44* high group also belonged to *CD44s* high group. Thus, in grade II/III gliomas, the mRNA expression level of *CD44s* could practically represent the mRNA expression level of total *CD44*. Then, we explored the clinical relevance of *CD44* mRNA expression based on the HUH cohorts, the TCGA cohorts, and the CGGA cohorts. In survival analysis, high mRNA expression of *CD44* was correlated with poor overall survival and poor progression-free survival in grade II/III glioma patients. Multivariate Cox regression analyses confirmed *CD44* as an independent prognostic factor for grade II/III glioma patients. According to GSEA, gene sets of Toll-like receptors (TLRs) signaling pathway, cell adhesion molecules, regulation of actin cytoskeleton, and chemokine signaling pathway are differentially enriched in *CD44* high expression phenotype.

Conclusions:

The study on key molecules in 5-ALA mediated FGS is the first, to the best of our knowledge, to demonstrate that PEPT2 is an important gene/protein in 5-ALA-mediated FGS in grade

II/III glioma. The overexpression of PEPT2 was associated with a higher fluorescence intensity of PpIX in grade II/III gliomas. These results may provide clues to improve the surgical treatment of grade II/III gliomas in the future.

The study on the prognostic significance of CD44 demonstrated that overexpression of *CD44* is correlated with a poor prognosis for grade II/III glioma patients. Our findings suggest that *CD44* could play an important role as a useful prognostic biomarker for grade II/III glioma patients.

List of Abbreviations

ALAD	aminolevulinate dehydratase
ALAS1	aminolevulinate synthase 1
ABCG2	ATP binding cassette subfamily G member 2
ABCB6	ATP binding cassette subfamily B member 6
BSA	bovine serum albumin
CGGA	Chinese Glioma Genome Atlas
CNS	central nervous system
CPOX	coproporphyrinogen oxidase
FDR	false discovery rate
FECH	Ferrochelatase
FGS	fluorescence-guided surgery
FPKM	fragments per kilobase per million mapped reads
GBM	glioblastoma multiforme
GSC	Glioma stem cell
GSEA	gene set enrichment analysis
HA	hyaluronan
HO1	heme oxygenase 1
HUH	Hokkaido University Hospital
IDH	isocitrate dehydrogenase
MRI	magnetic resonance imaging
NES	normalized enrichment score
OS	overall survival
PBS	phosphate-buffered saline
PEPT2	oligopeptide transporter 2
PFS	progression-free survival
PpIX	protoporphyrin IX
qPCR	quantitative real-time polymerase chain reaction
siRNA	small interfering RNA

TCGA	The Cancer Genome Atlas
TLR	Toll-like receptor
UROS	uroporphyrinogen III synthase
WHO	World Health Organization
5-ALA	5-aminolevulinic acid

Introduction

Glioma is the most frequent primary malignant brain tumor. Based on the World Health Organization (WHO) criteria, gliomas are classified into four grades (i.e., WHO grade I, II, III, and IV). Grade II/III gliomas are infiltrative tumors that occur most often in the cerebral hemispheres of adults (Ostrom et al., 2018). Surgery, combined with chemotherapy and radiotherapy, is the standard treatment; however, it remains incurable due to its high recurrence rate and invasiveness (Stupp et al., 2005). Even a subset of grade II/III gliomas will progress to glioblastoma multiforme (GBM, WHO grade IV gliomas) (Ostrom et al., 2018). Thus, studies on new therapeutic approaches and targets for grade II/III gliomas are of great importance. The present study mainly focused on two themes for grade II/III gliomas, potential molecular target for intraoperative diagnosis and the potential therapeutic target. Chapter 1 is the study on key molecules in 5-aminolevulinic acid (5-ALA) mediated fluorescence-guided surgery (FGS) in grade II/III gliomas and Chapter 2 is the study on the prognostic significance of CD44 in grade II/III gliomas.

Chapter 1. Studies on key molecules in 5-ALA mediated fuorescence-guided surgery in grade II/III gliomas

Introduction

Patients with glioma can benefit from the maximum safest resection (Lacroix et al., 2001; Sanai and Berger, 2008). However, surgeons often have difficulty distinguishing tumor tissue from normal tissue and in recognizing infiltrating glioma cells in normal tissues adjacent to tumor tissue intraoperatively. In addition, >90% of recurrent gliomas occur within 2–3 cm of the borders of the original tumor lesion (Aydin et al., 2001; Clarke et al., 2010; Theeler and Groves, 2011; Wallner et al., 1989).

In recent years, 5-aminolevulinic acid (5-ALA) fluorescence-guided surgery (FGS) appears to

be a promising treatment for glioma with documented survival benefits (Aldave et al., 2013; Stummer et al., 2006; Stummer et al., 1998). 5-ALA can be absorbed by glioma cells and then metabolized to Protoporphyrin IX (PpIX). Accumulated PpIX can lead to pronounced fluorescence when excited by violet–blue light, which assists in identifying the infiltrating area and increases the extent of tumor resection. However, the marginal region of tissue containing infiltrating glioma cells exhibits vague fluorescence due to insufficient PpIX accumulation (Utsuki et al., 2006). In addition, 5-ALA-mediated fluorescence cannot be detected in all cases, particularly in the World Health Organization (WHO) grade II/III gliomas (Jaber et al., 2016).

The molecular mechanisms underlying the accumulation of PpIX mediated by 5-ALA remain to be fully clarified. If the mechanisms can be elucidated, the fluorescence intensity mediated by 5-ALA in glioma may be managed by surgeons, and guide future maximum resection.

Compared with glioblastoma multiforme (GBM), a higher proportion of grade II/III cases do not exhibit 5-ALA-mediated fluorescence in tumor tissue. Therefore, the present study aimed to investigate the gene expression patterns of the PpIX synthesis pathway according to the 5-ALA-mediated fluorescence status of grade II/III gliomas, and then identify the candidate molecules influencing the fluorescence.

Methods and Materials

Surgical excision of glioma specimens

Since 2008, every patient who had suspected glioma in Hokkaido University Hospital (Sapporo, Japan) was administered with 5-ALA (20 mg/kg, COSMO, Japan) orally 2–3 h prior to surgery. The fluorescence mediated by 5-ALA was visualized under a surgical microscope (OPMI-Pentero; Carl Zeiss) with high-powered, violet–blue LED light (CCS, Inc., Kyoto, Japan) during surgery. Surgically obtained glioma specimens emitting deep-red fluorescence or pink fluorescence were classified as fluorescence-positive. By contrast, glioma specimens without fluorescence were classified as fluorescence-negative. The

fluorescence intensity status of each specimen was discussed and evaluated by two neurosurgeons (S.Y. and H.K.) during the procedure and recorded in the surgical records. If no fluorescence was detected in the tumor tissue, the tissue was cryopreserved and classified as fluorescence-negative. If fluorescence was partly detected in the excised tumor tissue, the fluorescing region was cryopreserved and the tissue was classified as fluorescence-positive. The surgical specimens were cryopreserved at -80˚C. This study was approved by the local Ethics Committee at Hokkaido University Hospital (Sapporo, Japan; 017-0032). All procedures performed in the present study were in accordance with 1964 Helsinki Declaration and its later amendments.

In the present study, surgical specimens from our archives were selected according to the following criteria: (1) obtained at primary tumor resection without any adjuvant therapy, including chemotherapy or radiotherapy; (2) histologically diagnosed as grade II or III gliomas based on WHO 2007 criteria, which included diffuse astrocytoma, oligodendroglioma, oligoastrocytoma, anaplastic astrocytoma, anaplastic oligodendroglioma, and anaplastic oligoastrocytoma; classification and pathologic diagnosis of gliomas were made by a certified pathologist; (3) cryopreserved tissue samples were assigned to a corresponding intraoperative fluorescence status. The mutation status of isocitrate dehydrogenase (IDH) was also investigated. Mutation hotspots at codon 132 of IDH1 and codon 172 of IDH2 were screened using Sanger sequencing. In addition, 1p/19q loss of heterozygosity status was analyzed using a multiplex ligation-dependent probe amplification procedure. The tumors were re-diagnosed according to the WHO 2016 criteria according to the IDH and 1p19q status. In addition, all patients received magnetic resonance imaging (MRI) with contrast enhancement preoperatively. According to the enhancement pattern, the tumors were classified as enhanced tumors and non-enhanced tumors. Tumors that exhibited apparent enhancement, including a heterogeneous or ring-like pattern, were defined as an enhanced tumor. Tumors without obvious enhancement were defined as a non-enhanced tumor.

Quantitative real-time polymerase chain reaction (qPCR) analysis

As a control reference, two sets of commercially available human brain total RNA were obtained (Life Technologies; Clontech). The glioma total RNA was extracted from the frozen specimens using an All Prep DNA/RNA Mini kit (QIAGEN) based on the manufacturer's instructions. cDNA was synthesized from total RNA using the PrimeScript™ II 1st Strand cDNA Synthesis kit (Takara Biotechnology Co., Ltd., Dalian, China). Several genes within the PpIX synthesis pathway were selected, including *ALAD, ALAS1, ABCG2, ABCB6, CPOX, FECH, HO-1, PEPT2,* and *UROS*, to identify candidate molecules in 5-ALA-mediated grade II/III glioma fluorescence. The gene primers are listed in Table 1. Reverse transcription-qPCR analysis was performed with LightCycler 96 (Roche Diagnostics, Basel, Switzerland) and the PCR product specificities were confirmed via melt curve analysis. To normalize the target transcript, *GAPDH* was used, which is one of the most stably expressed housekeeping genes for endogenous control. The PCR experiments were run in triplicate. The -ΔΔCT equation was applied to calculate the relative expression of tumor samples with the average value of the normal brain as a reference control.

Table 1. Quantitative real-time polymerase chain reaction primers of genes in protoporphyrin IX synthesis pathways.

Gene	F/R	Primer Sequence 5'to 3'
ALAD	Forward	CTTGGCAACAGGGTATCGGT
	Reverse	AGCTGGGCTTGACTTAGCTG
ALAS1	Forward	CCTAGATTCTTTCCACAGGAGCC
	Reverse	CATCTTGGGGCAGTTTTGGG
ABCG2	Forward	AGTTCTCAGCAGCTCTTCGG
	Reverse	TTCCAACCTTGGAGTCTGCC
ABCB6	Forward	CTGCGGTATGTGGTCTCTGG
	Reverse	GAACCTGGCTCCTTTCCACA
CPOX	Forward	ATCTGCTGTATGATCGGGGC
	Reverse	ACTCCCATCGGGCAGTTAGA
FECH	Forward	TCAACCGCAGAAGAGGAAGC
	Reverse	TGTCATGAGGTCTCGGTCCA
HO-1	Forward	AAGACTGCGTTCCTGCTCAA
	Reverse	GGGGGCAGAATCTTGCACTT

PEPT2	Forward	CTCCAGGCAGCTTGGCTATT
	Reverse	GAATTCGGCCCACTGTACCA
UROS	Forward	GCGCTCAAGGACAAAGGGAT
	Reverse	TGTGAGGCCAGAGGGACTAA

ALAD (ALA dehydratase), *ALAS1* (ALA synthase 1), *ABCG2* (ATP Binding Cassette subfamily G member 2), *ABCB6* (ATP Binding Cassette subfamily B member 6), *CPOX* (Coproporphyfinogen oxidase), *FECH* (Ferrochelatase), *HO-1* (heme oxygenase 1), *PEPT2* (oligopeptide transporter 2), *UROS* (uroporphyrinogen III synthase).

Immunofluorescence analysis.

The protein expression of PEPT2 was detected by immunofluorescence staining using the paraffin-embedded tumor sections. The sections were incubated with rabbit polyclonal PEPT2 antibody (Abcam, 1:100) as the primary antibody in 0.5% bovine serum albumin (BSA) for 1 h at room temperature. Phosphate-buffered saline (PBS) was used in the negative control instead of the primary antibody. Alexa Fluor® 594 goat anti-rabbit antibody (Life Technologies, 1:200) in 0.5% BSA was used as the secondary antibody. The nuclei were stained with DAPI (Invitrogen). Staining was observed using the KEYENCE BZ-X700 fluorescence microscope with a 20X objective.

Western blot analysis

The proteins were extracted from five fluorescence-negative grade II/III gliomas and five fluorescence-positive grade II/III gliomas. The proteins were loaded on a Blot™ 4%–12% Bis–Tris Plus gel (Invitrogen™), electrophoresed, and fractionated at 200 V for 30 min in SDS running buffer, and then transferred onto a 0.2-μm-pore nitrocellulose membrane (Invitrogen™). Following blocking with 2% ECL Prime blocking agent (GE Healthcare) in PBS-Tween 20 for 1 h at room temperature, the membrane was incubated with primary antibodies against PEPT2 (Abcam,1:500) and β-actin (Santa Cruz Biotechnology, Inc., 1:1,000) with gentle shaking at 4˚C overnight, followed by incubation with a horseradish peroxidase-conjugated, goat anti-mouse secondary antibody (Santa Cruz Biotechnology, Inc., 1:5,000) or goat anti-rabbit secondary antibody (Santa Cruz Biotechnology, Inc., 1:5,000) at room temperature for 2 h. Finally, the proteins were visualized using the enhanced

chemiluminescence method (Bio-Rad Laboratories, Inc., Hercules, CA, USA).

RNA interference experiments

The commercially available SW-1783 human grade III glioma cell line (ATCC®) was used in the present study. The SW-1783 cells were maintained in DMEM-high glucose (NacalaiTesque), supplemented with 10% fetal bovine serum (FBS, Life Technologies), in a 5% CO_2-humidified incubator at 37˚C. The SW-1783 cells were plated in 6-well plates. Each well of cells was transfected with 2,500 ng of *PEPT2* Silencer® Select Pre-designed small interfering (si)RNA (cat. no. s13065, Life Technologies) or Silencer® Select Negative Control #1 siRNA (Life Technologies) using Lipofectamine 3000 (Invitrogen™) according to the manufacturer's instructions. The cells were harvested 24 h following transfection and subjected to RT-qPCR and western blot analyses to examine the silencing efficiency.

PpIX fluorescence spectrum analysis

The cells were randomly divided into four groups: Negative control (NC) siRNA, NC siRNA + 5ALA, *PEPT2* siRNA, and *PEPT2* siRNA + 5ALA. The 5-ALA (Cosmo Bio) was stored at 4˚C in the dark and dissolved in DMEM-high glucose (NacalaiTesque), supplemented with 10% FBS, to a final concentration of 200 μg/ml. For the NC + 5ALA group and the *PEPT2* siRNA + 5ALA group, the culture medium was replaced with a medium containing 5-ALA 24 h following transfection, followed by incubation for 4 h at 37˚C. For the NC siRNA group and *PEPT2* siRNA group, the culture medium was replaced with fresh DMEM-high glucose, supplemented with 10% FBS without 5-ALA, at 24 h post-transfection. Following incubation for 4 h, the cells were washed with PBS (NacalaiTesque) and collected using 0.05% trypsin with 0.5 mM ethylenediaminetetraacetic acid in 15-mL conical tubes (FALCON®). The liquid supernatant was discarded following centrifugation at 1,000 revolutions per min. The fluorescence spectrum was detected by VLD-EX (SBI Pharma) in the dark room. Subsequently, the illuminant with optical fiber was placed into the 15-mL conical tubes. The distance between the bottom of the conical tube and the illuminant was maintained at ~2 cm. The excitation wavelength was 406 nm. Visual images were captured using a camera (ILCE-A5000, Sony). The quantified fluorescence spectrum was presented on the screen of the VLD-EX machine.

Statistical analysis

SPSS 22.0 and R statistical software, version 3.4.1, were used to conduct all statistical analyses. Continuous variables were compared using the one-way analysis of variance. The Least Significant Difference test was used to compare differences between groups. Categorical variables are expressed as frequency (percentage) and were compared using the Chi-square ($\chi 2$) test. $P < 0.05$ was considered to indicate a statistically significant difference. Hierarchical clustering analysis, presented as a heat map, was performed using R software to demonstrate the distinguishable mRNA expression profiles among the samples. "hclust" was used to compute the hierarchical clustering analysis, with the Ward method as the method of clustering, and the Euclidean distance as the distance metric. The results were visualized using dendrograms and heat maps.

Results

Patient characteristics

A total of 50 grade II/III glioma specimens, including grade II (N = 22) and grade III (N = 28) specimens, were matched to the above criteria. The tumors were re-diagnosed according to the WHO 2016 criteria. The types and the numbers of the grade II and grade III gliomas are listed in Table 2.

Table 2. Tumor types and numbers of the cases in this study.

Tumor type	Number of cases
Diffuse astrocytoma	12
Oligodendroglioma	10
Anaplastic astrocytoma	15
Anaplastic oligodendroglioma	13

The numbers of cases in terms of the grade of the glioma and 5-ALA-mediated fluorescence status are listed in Table 3. In the grade II gliomas, only 2/22 cases (9%) were detected with fluorescence. By contrast, in the grade III gliomas, 19/28 cases (68%) were detected with

fluorescence and 9 cases (32%) showed no fluorescence. The fluorescence status was significantly influenced by histological malignancy ($p<0.001$).

Table 3. 5-ALA-mediated fluorescence status in relation to the grading of 50 grade II/III gliomas.

Fluorescence status	Grade II glioma	Grade III glioma	Total
Fluorescence-positive	2	19	21
Fluorescence-negative	20	9	29
Total	22	28	50

5-ALA, 5-aminolevulinic acid; FGS, fluorescence-guided surgery.

The correlation between IDH status and 5-ALA-mediated fluorescence status is shown in Table 4. Gliomas with IDH mutations were predominantly fluorescence-negative (25/36 cases; 69%), whereas gliomas without IDH mutations were predominantly fluorescence-positive (10/14 cases; 71%). The difference was statistically significant ($p = 0.009$).

Table 4. 5-ALA-mediated fluorescence status in relation to the IDH status of 50 grade II/III gliomas.

Fluorescence status	IDH mutant glioma	IDH wild-type glioma	Total
Fluorescence-positive	11	10	21
Fluorescence-negative	25	4	29
Total	36	14	50

5-ALA, 5-aminolevulinic acid; IDH, isocitrate dehydrogenase.

The correlations between MRI contrast enhance status and the 5-ALA-mediated fluorescence status of the tumors are shown in Table 5. The non-enhanced tumors were predominantly fluorescence-negative (23/34 cases; 68%), and the difference was statistically significant ($p = 0.044$).

Table 5. 5-ALA FGS fluorescence status in relation to MRI contrast enhance status of the 50 grade II/III

gliomas.

	MRI enhanced	MRI Non-enhanced	Total
Fluorescence-positive	10	11	21
Fluorescence-negative	6	23	29
Total	16	34	50

mRNA expression of genes in the PpIX synthesis pathway

The relative mRNA expression levels, according to 5-ALA-mediated fluorescence status, are shown in Fig. 1. Compared with those in the normal brain, the mRNA expression of levels of *ABCG2* ($p < 0.05$), *ABCB6* ($p < 0.05$), and *HO-1* ($p < 0.05$) were significantly higher in the fluorescence-negative grade II/III gliomas, and the mRNA expression levels of *PEPT2* ($p < 0.05$), *ABCG2* ($p < 0.01$), *ABCB6* ($p < 0.01$), and *HO-1* ($p < 0.001$) were significantly higher in the fluorescence-positive grade II/III gliomas. Compared with the fluorescence-negative grade II/III gliomas, the mRNA expression levels of *PEPT2* ($p < 0.05$), *ALAD* ($p < 0.01$), *ABCG2* ($p < 0.05$), *ABCB6* ($p < 0.01$), *CPOX* ($p < 0.05$), *HO-1* ($p < 0.05$), and *UROS* ($p < 0.001$) were also significantly higher in the fluorescence-positive gliomas. There were no significant differences in the mRNA expression of *ALAS1* or *FECH* between the groups.

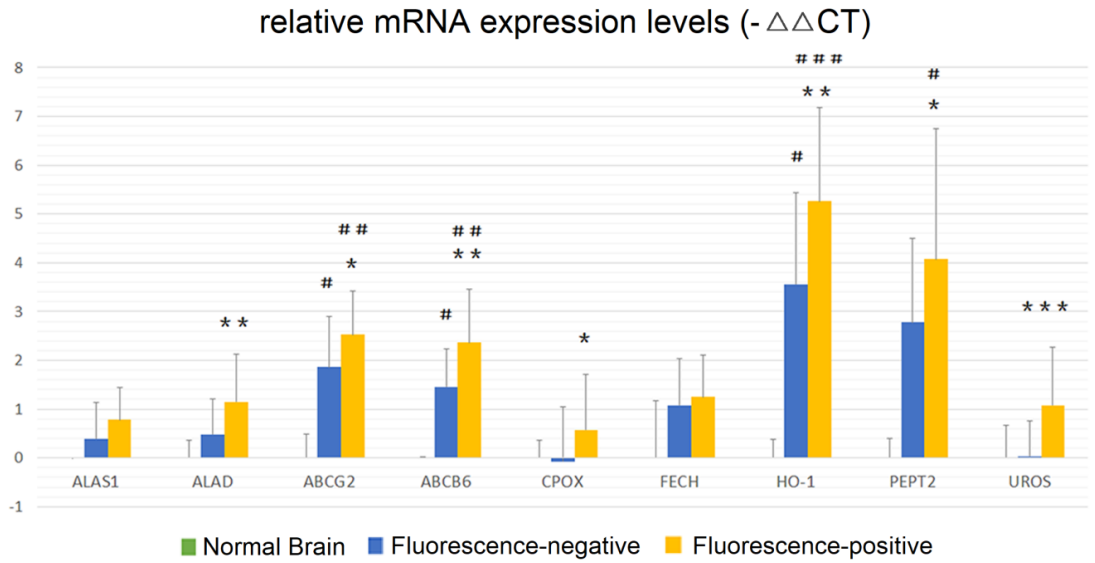

Figure 1. Relative mRNA expression levels of *ALAS1*, *ALAD*, *ABCG2*, *ABCB6*, *CPOX*, *FECH*, *HO-1*, *PEPT2*, and *UROS* of all grade II/III gliomas in three groups. Data are presented as the mean ± standard error of the mean with three replicates for each glioma specimen. #P<0.05 compared with the normal brain group, ##P<0.01 compared with the normal brain group, ###P<0.001 compared with the normal brain group, *P<0.05 compared

with the fluorescence-negative group, **P<0.01 compared with the fluorescence-negative group, *** P<0.001 compared with the fluorescence-positive group.

According to the PpIX synthesis pathway (Fig. 2), PEPT2 is responsible for transporting 5-ALA and PEPT2 is an upstream molecule in the PpIX synthesis pathway. Therefore, the data obtained suggested that the overexpression of PEPT2 affected the fluorescence intensity mediated by 5-ALA in grade II/III gliomas. The present study also compared the mRNA expression of *PEPT2* between MRI enhanced grade II/III gliomas and MRI non-enhanced grade II/III gliomas. The mRNA expression of *PEPT2* in the enhanced tumors was higher than that in the non-enhanced tumors, although this difference did not reach statistical significance (data not shown).

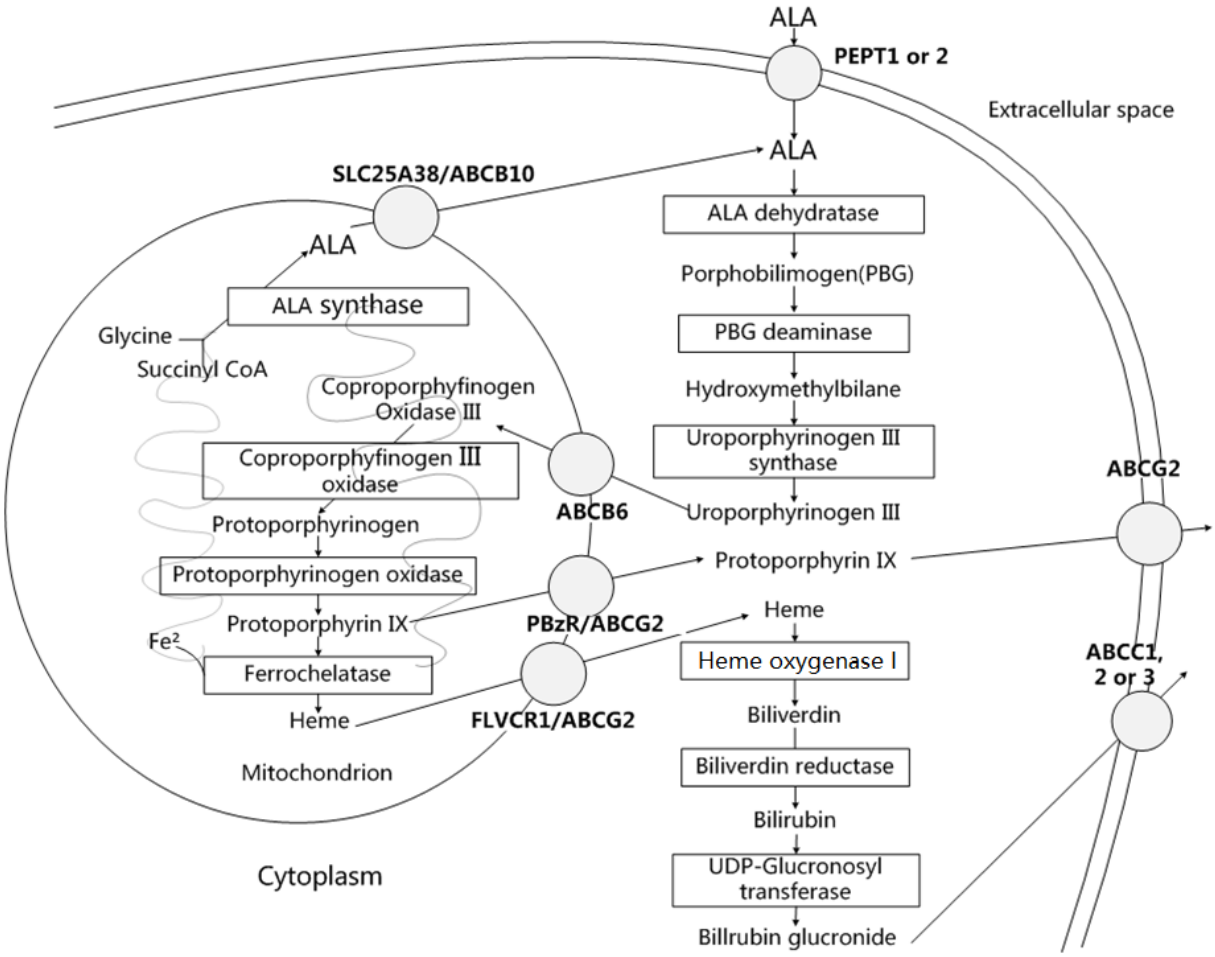

Figure 2. PpIX/heme biosynthesis and metabolic pathway. Multiple enzymes and transporters are involved in this pathway. The enzymes are marked with rectangles. ABCB10, ATP Binding cassette subfamily B member 10; ABCC1, 2 or 3, ATP binding cassette subfamily C member 1, 2 or 3; PBzR, peripheral benzodiazepine receptor; FLVCR1, feline leukemia virus subgroup c receptor 1; SLC25A38, solute carrier family 25 member 38.

Hierarchical clustering of the expression patterns demonstrated there are two major clusters (Fig. 3). Cluster 1 contained 19 tumors, and cluster 2 contained 31 tumors. In terms of the 5-ALA-mediated fluorescence status, the majority of fluorescence-negative tumors (16/28 tumors; 57%) and three of the 21 fluorescence-positive tumors (14%) belonged to cluster 1. The majority of the fluorescence-positive tumors (18/21 tumors; 86%) belonged to cluster 2. In addition, in terms of the IDH status, cluster 1 consisted of almost IDH mutant grade II/III gliomas. In terms of MRI contrast enhancement status, only one of the 16 MRI contrast enhanced tumors (6%) belonged to cluster 1.

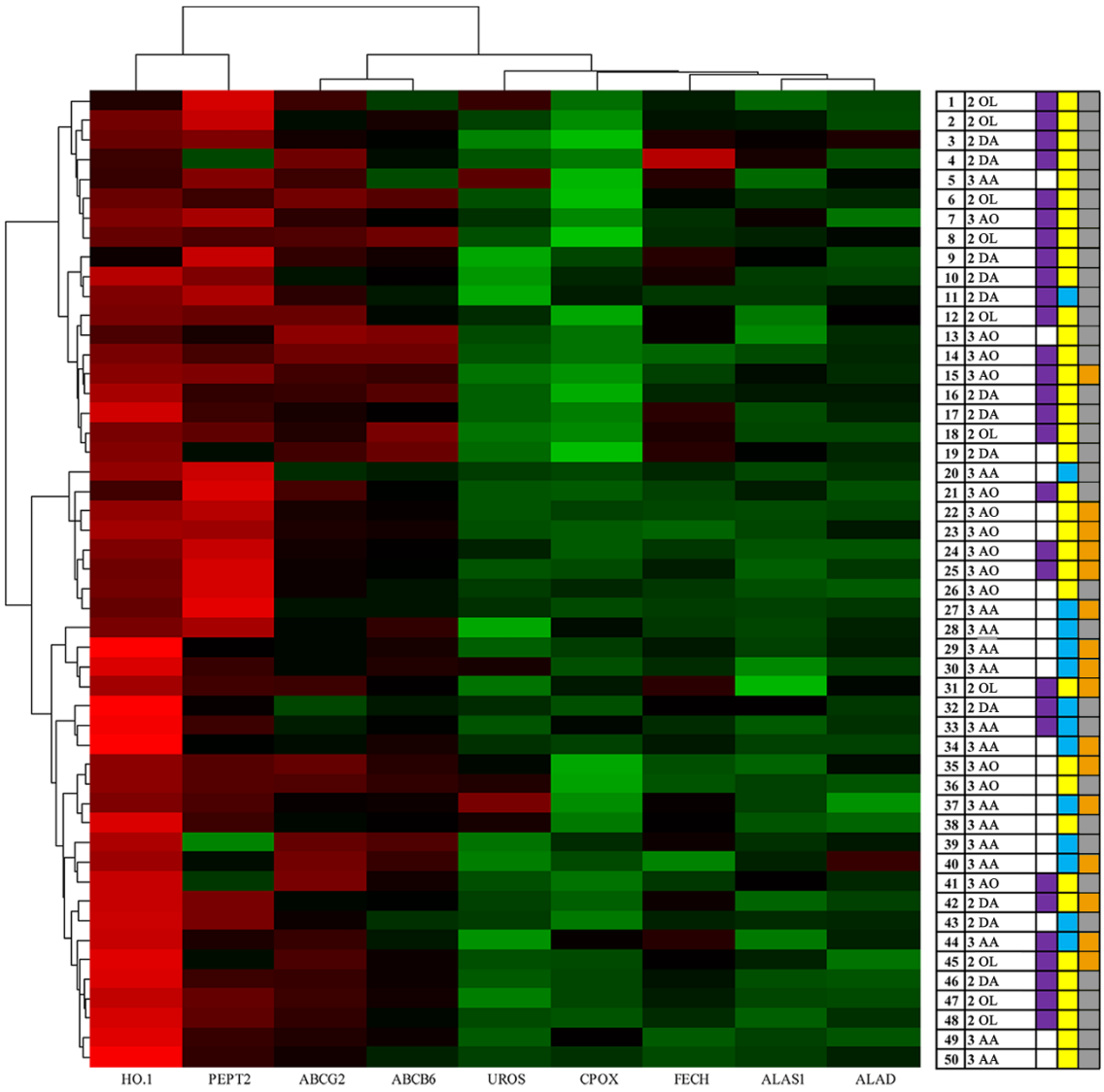

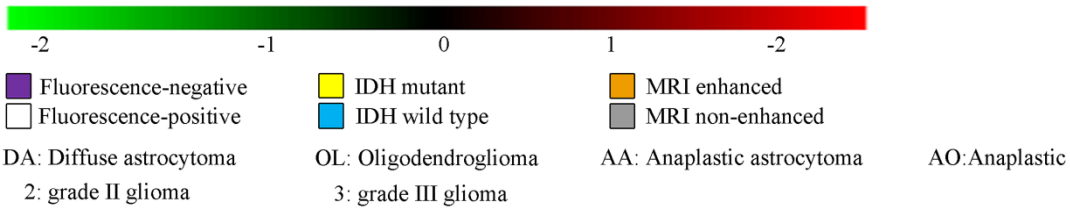

Figure 3. Heat map summary and hierarchical clustering for *ALAD*, *ALAS1*, *ABCG2*, *ABCB6*, *CPOX*, *FECH*, *HO-1*, *PEPT2*, and *UROS* of the 50 specimens. Samples are depicted in rows and RNAs are depicted in columns. Red indicates high expression, and green indicates low expression.

Protein expression of PEPT2 measured by immunofluorescence and western blot analysis

According to the results of the RT-qPCR analysis of the PpIX synthesis pathway, the present study focused on the overexpression of PEPT2, as it may be important in the accumulation of PpIX following the administration of 5-ALA in grade II/III gliomas. PEPT2, also known as SLC15A2, is widely expressed in glial cells and mediates the uptake of peptide substrates. PEPT2 polyclonal antibody was used to detect protein expression by immunofluorescence in fluorescence-positive grade II/III gliomas and fluorescence-negative grade II/III gliomas. The immunofluorescence results of three fluorescence-positive cases and three fluorescence-negative cases are shown in Fig. 4. Compared with the fluorescence-negative grade II/III gliomas, a higher expression of PEPT2 was present in the fluorescence-positive grade II/III gliomas.

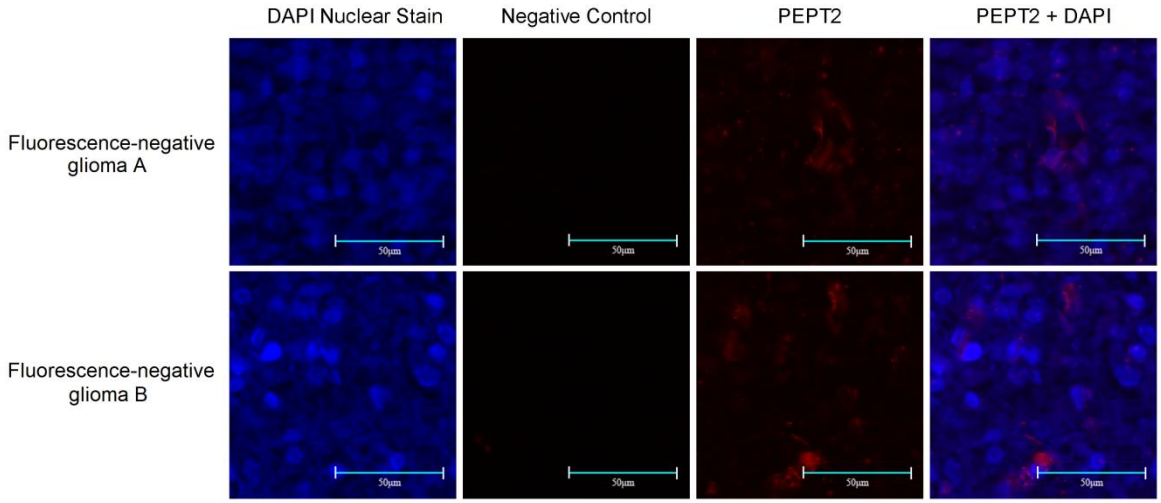

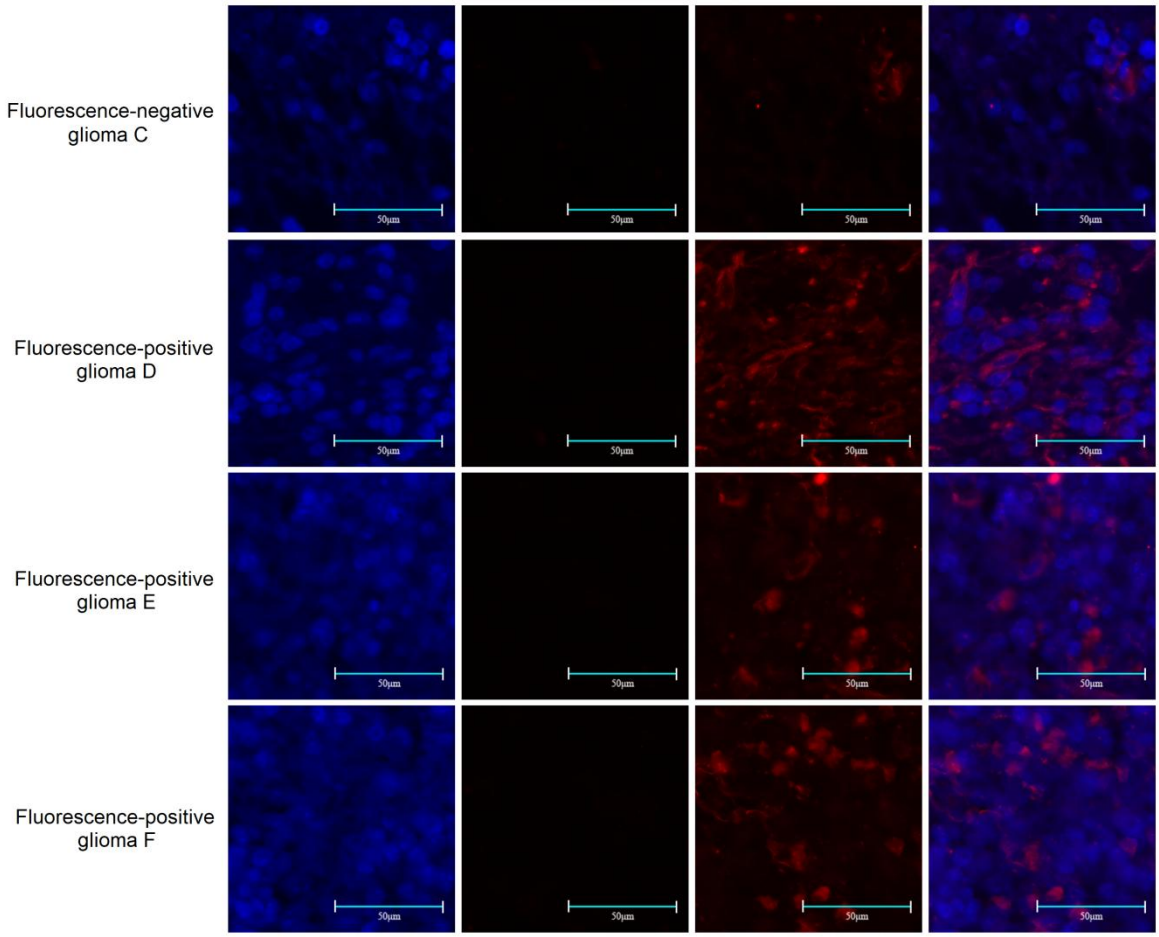

Figure 4. Protein expression of PEPT2 measured by immunofluorescence analysis and western blot analysis. **a** Protein expression of PEPT2 measured by immunofluorescence analysis. PBS was used in negative control instead of primary antibody. PEPT2 protein was detected with Alexa Fluor® 594 goat anti-rabbit secondary antibody (red). Nuclei were stained with DAPI (blue). Protein expression of PEPT2 in fluorescence-positive grade II/III gliomas was higher than in fluorescence-negative grade II/III gliomas.

The present study also investigated the relative protein expression levels of PEPT2 and compared them between five fluorescence-negative grade II/III gliomas and five fluorescence-positive grade II/III gliomas using western blot analysis. Consistent with the product datasheet of primary PEPT2 antibody, bands at a size of 90 kDa were observed, and the predicted band was identified at a size of 82 kDa. The results (Fig. 5) demonstrated that the protein expression of PEPT2 in the fluorescence-positive grade II/III gliomas was significantly higher than that in the fluorescence-negative grade II/III gliomas ($p < 0.01$). These results revealed that the overexpression of PEPT2 might be important in the 5-ALA-mediated PpIX fluorescence intensity of gliomas.

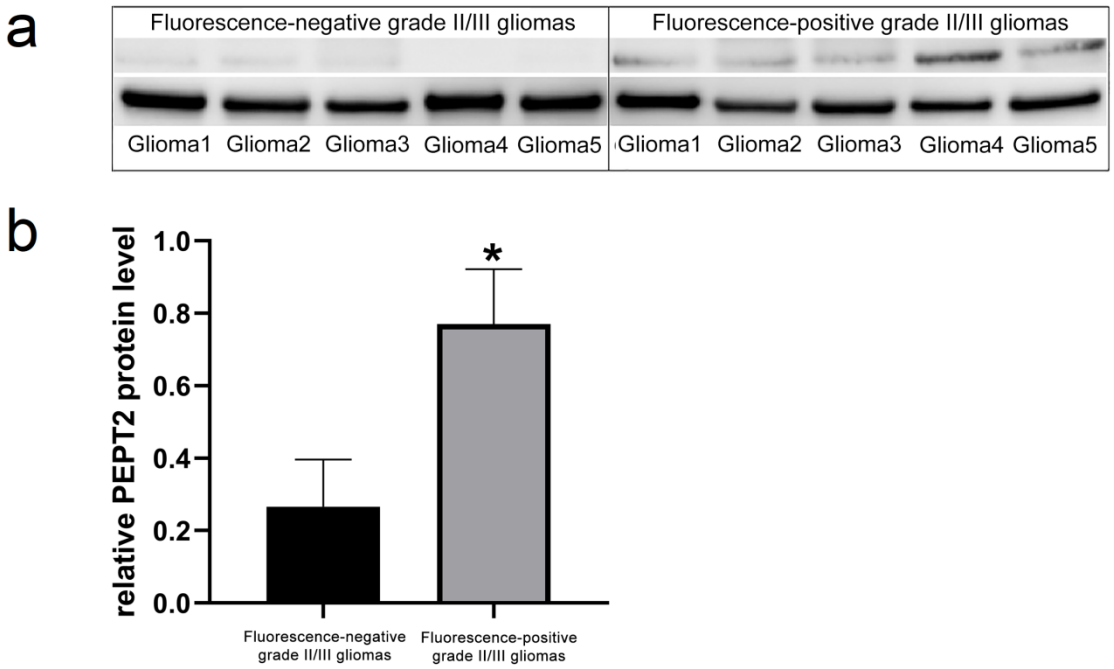

Figure 5. Protein expression of PEPT2 measured by western blot analysis. **a** Western blotting of five fluorescence-positive grade II/III gliomas and five fluorescence-negative grade II/III gliomas using antibody against PEPT2. β-actin was used as a loading control. **b** Comparison of relative protein expression levels of PEPT2 between five fluorescence-positive grade II/III gliomas and five fluorescence-negative grade II/III gliomas based on densitometric analysis of western blots. Data are presented as the mean ± standard error of the mean of three replicates for each glioma specimen. *$p<0.05$ compared with the fluorescence-negative grade II/III gliomas.

RNA interference and PpIX fluorescence spectrum analysis.

In order to further confirm the exact function of PEPT2, the present study aimed to inhibit the expression of PEPT2 in the SW-1783 cell line using siRNA. Protein expression was successfully downregulated by ~50% at 24 h post-transfection with specific siRNA (Fig. 6a to c). The fluorescence spectrums of the four groups (NC siRNA + 5ALA, NC siRNA, *PEPT2* siRNA + 5ALA, and *PEPT* siRNA) were detected using VLD-EX in the dark room. The peak wavelength of 636 nm represents the PpIX fluorescence spectrum. The results demonstrated that the downregulation of PEPT2 led to decreased fluorescence intensity (Fig. 6d and e) in the SW-1783 cells. This result suggested that 5-ALA-mediated fluorescence may be influenced by the expression of PEPT2 in grade II/III gliomas.

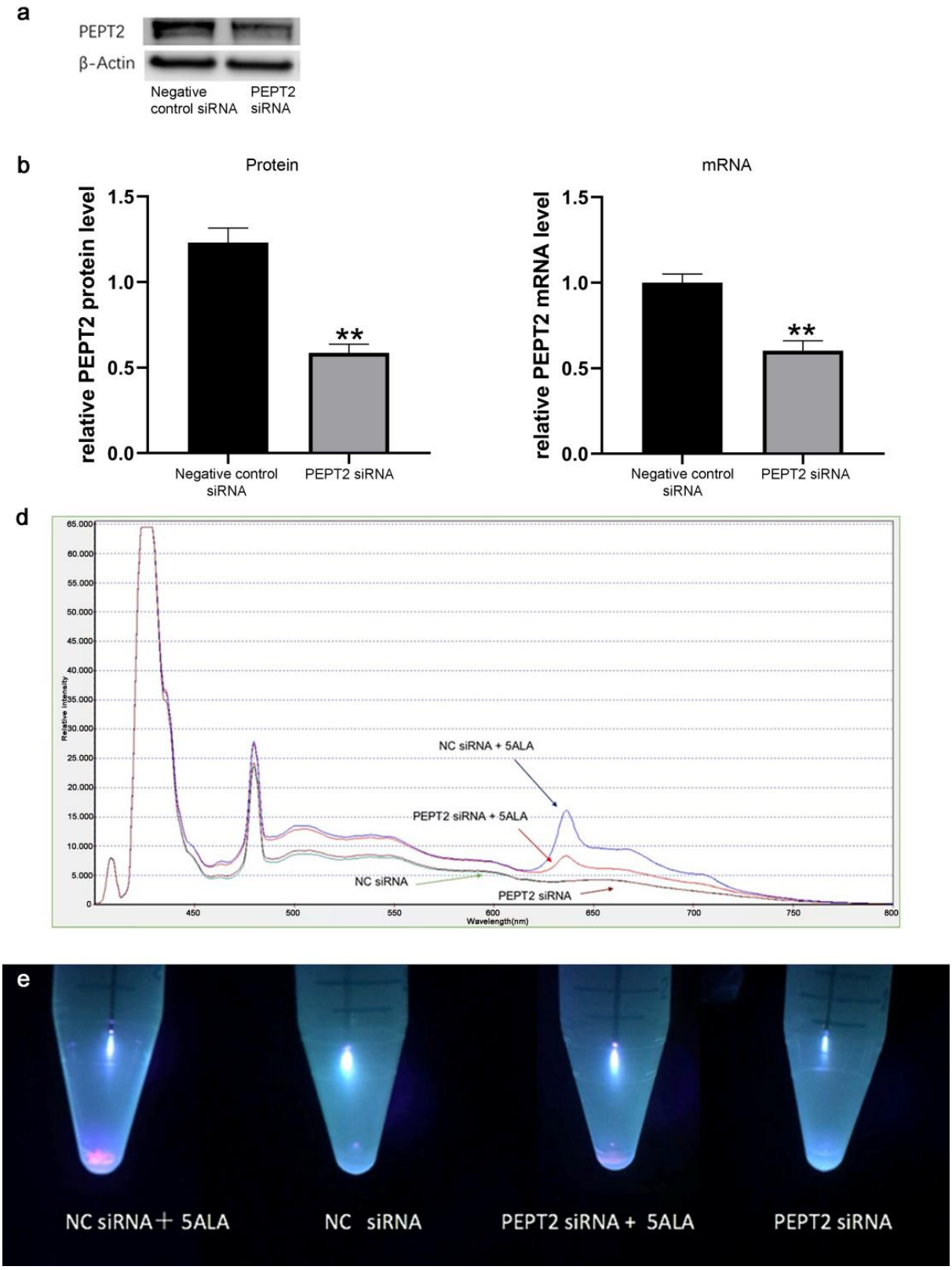

Figure 6. RNA interference experiments and PpIX fluorescence spectrum analysis. **a** Western blotting of SW-1783 cells transfected with PEPT2 siRNA or negative control siRNA using antibody against PEPT2. β-actin was used as a loading control. **b** Semi-quantitative analysis of western blots. Data are presented as the mean ± standard error of the mean of three replicates for each experimental condition. **c** mRNA expression of PEPT2 in

SW-1783 cells transfected with PEPT2 siRNA or negative control siRNA.**p<0.01 compared with SW-1783 cells transfected with negative control siRNA. **d** PpIX fluorescence spectrum of the four groups (NC siRNA + 5ALA, NC siRNA, PEPT2 siRNA + 5ALA, and PEPT2 siRNA). **e** Visual images of the fluorescence of PpIX in the four groups. The density of cells in each sample was ~$1x10^6$.

Discussion

Patients with glioma may benefit from the maximum safe tumor resection (Lacroix et al., 2001; Sanai and Berger, 2008). However, surgeons may have difficulty distinguishing tumor tissue from normal tissue during surgery. 5-ALA-mediated FGS has become a useful surgical technique in glioma resection and improves the overall survival rate of patients with malignant glioma (Aldave et al., 2013; Stummer et al., 2006; Stummer et al., 1998). However, fluorescence cannot be detected in all cases of glioma, particularly in lower-grade tumors (Jaber et al., 2016). In the present study, in the grade II gliomas, only 2/22 cases (9%) were detected with fluorescence. By contrast, in the grade III gliomas, 19/28 cases (68%) were detected with fluorescence and 9 cases (32%) showed no fluorescence (Table 1). Therefore, the 5-ALA-mediated FGS in grade II/III gliomas may be useful.

The FGS mechanism mediated by 5-ALA in gliomas remains to be fully elucidated. In particular, compared with GBMs, there has been no previous investigation of the molecular mechanism underlying 5-ALA-mediated FGS in lower-grade glioma. Fluorescence-positive and fluorescence-negative cases may show different gene expression patterns. Therefore, the present study was performed to investigate the differences in gene expression patterns between fluorescence-positive grade II/III gliomas and fluorescence-negative grade II/III gliomas. If the underlying genetic mechanism of the fluorescence of PpIX mediated by 5-ALA can be clarified, the fluorescence intensity may be managed by neurosurgeons in the future.

The present study first attempted to identify candidate genes with an effect on 5-ALA-mediated PpIX fluorescence intensity. The mRNA expression levels of genes in the PpIX synthesis pathway were compared among normal brain tissues, fluorescence-negative

grade II/III gliomas, and fluorescence-positive grade II/III gliomas. The results demonstrated that mRNA expression levels of *ALAD* ($p < 0.01$), *ABCG2* ($p < 0.05$), *ABCB6* ($p < 0.01$), *CPOX* ($p < 0.05$), *HO-1* ($p < 0.05$), *PEPT2* ($p < 0.05$), and *UROS* ($p < 0.001$) were significantly higher in the fluorescence-positive grade II/III gliomas than the fluorescence-negative grade II/III gliomas (Fig. 1).

Among the above candidate genes, the present study focused on PEPT2 as it is an upstream molecule in the PpIX synthesis pathway (Fig. 2). In the central nervous system (CNS), PEPT2 can remove peptide/mimetic drugs from the cerebrospinal fluid to the plasma. PEPT2 is also responsible for the uptake of peptide/mimetic drugs from brain extracellular fluid into brain cells, which is important in regulating drug metabolism in the CNS (Chen et al., 2017; Hu et al., 2005; Novotny et al., 2000).

PEPT2 protein consists of 729 amino acids, and the core molecular size is 81,940 Da. PEPT2 is a high-affinity and low-capacity transporter, which is widely expressed in the brain, lung, kidney, eye, and mammary gland (Daniel and Kottra, 2004; Liu et al., 1995). PEPT2 is located in the cell membrane and is responsible for the selective transportation of peptides, amino acids, and drugs (Rubio-Aliaga and Daniel, 2002; Terada and Inui, 2004; Terada et al., 2000). PEPT1 and PEPT2 are responsible for 5-ALA uptake. However, the affinity of PEPT2 to the same substrates is higher than that of PEPT1, which is mainly expressed in the intestine (Doring et al., 1998; Wang et al., 2010). In general, >400 dipeptides and 8,000 tripeptides, including 20 essential L-α-amino acids and the majority of D-enantiomers, can be sequence-independently transported by PEPT2. In addition, numerous peptide-like drugs, including β-lactam antibiotics, angiotensin-converting enzyme inhibitors, and peptidase inhibitors can be mediated and transported by PEPT2 substrate (Rubio-Aliaga and Daniel, 2002; Terada et al., 2000; Verrey et al., 2009).

Previous functional investigations of PEPT2 have focused predominantly on its transportation and absorption effect. In the kidney, PEPT2 is almost entirely responsible for the reabsorption of peptides and peptidomimetics (Rubio-Aliaga and Daniel, 2002; Sala-Rabanal et al., 2008;

Shen et al., 2007; Verrey et al., 2009). PEPT2 in the lung is located in alveolar type II pneumocytes, the bronchial epithelium, and the endothelium of small vessels, and is responsible for delivering peptides and peptidomimetics (Groneberg et al., 2001; Gukasyan et al., 2017). Of note, it has been demonstrated that PEPT2-null mice are fertile and healthy. Therefore, the exact function of PEPT2 requires further investigation (Frey et al., 2006; Rubio-Aliaga et al., 2003).

In the present study, it was hypothesized that PEPT2 may be key in the uptake of 5-ALA and 5-ALA-mediated PpIX fluorescence in grade II/III gliomas. The protein expression of PEPT2 was between fluorescence-negative grade II/III gliomas and fluorescence-positive grade II/III gliomas. The results demonstrated that the protein expression of PEPT2 in fluorescence-positive grade II/III gliomas was significantly higher than that in fluorescence-negative grade II/III gliomas ($p < 0.05$), which suggested that the levels of PEPT2 may affect the fluorescence intensity of PpIX. To further investigate the exact function of PEPT2, the mRNA and protein expression of PEPT2 were inhibited in a grade III glioma cell line and the PpIX fluorescence spectrum was detected. The results demonstrated that the downregulation of PEPT2 decreased fluorescence intensity. These findings suggest that the expression of PEPT2 is important for the 5-ALA-mediated fluorescence intensity of PpIX.

Previous studies have demonstrated that the overexpression of ABCB6 can enhance the 5-ALA-mediated fluorescence of PpIX in human glioma (Zhao et al., 2013). ABCB6 is a transporter in the PpIX metabolic pathway. This result is consistent with the RT-qPCR results in the present study, which showed that the mRNA of *ABCB6* was overexpressed in fluorescence-positive grade II/III gliomas. In a study conducted by Takahashi *et al* (Takahashi et al., 2011), the mRNA expression levels of *PEPT2, ABCB, and ABCG2* appeared to be relatively lower in samples with a high level of fluorescence, which is inconsistent with the results of the present study. This may be due to the samples used in the previous study being glioblastomas and metastatic brain tumors, which may exhibit gene expression patterns distinct from those of grade II/III gliomas. Hu e*t al* found that PEPT2 reduced the

neurotoxicity of 5-ALA (Hu et al., 2007), which indicates that the expression of PEPT2 may also influence the efficacy of 5-ALA-mediated photodynamic therapy. This also suggests that PEPT2 is important in glioma treatment. Therefore, future studies may examine the role of PEPT2 in glioma photodynamic therapy.

Chapter 2. Studies on the prognostic significance of CD44 in grade II/III gliomas

Introduction

The study in Chapter 1 focused on the key molecules and molecular mechanisms underlying 5-ALA mediated fluorescence-guided surgery. This may do help to provide clues and new ideas to improve the surgical treatment of grade II/III gliomas in the future. At the same time, also based on grade II/III gliomas, we investigated in the candidate therapeutic targets for grade II/III gliomas, which might be also important for treatment for patients with glioma in the future.

Based on the World Health Organization (WHO) criteria, gliomas are classified into four grades. Glioblastoma (GBM), is considered a grade IV tumor and accounts for 50 percent of all gliomas (Ostrom et al., 2018). GBM is the most aggressive type of brain tumor in adults. Despite surgery and post-operative chemotherapy and radiotherapy, the median survival is only 14.6 months (Stupp et al., 2005). Glioma stem cells (GSCs) are considered to be largely responsible for the poor prognosis in GBM (Auffinger et al., 2015).

CD 44 is a major cell surface receptor for hyaluronan (HA) and many other extracellular matrix components, and is implicated in cell adhesion, cell migration, and signaling (Ponta et al., 2003). The concentrations of HA in malignant tumors are usually higher than that are seen in the corresponding benign or normal tissues, and the high expression levels of HA contribute to tumor proliferation, progression, and metastasis (Toole, 2004). Overexpression of HA is correlated with poor prognosis in many cancers (Tammi et al., 2008), suggesting that CD44 might be important in tumor progression, and migration. There are two families of CD44 isoforms: 1) the standard isoform of CD44 (CD44s); and 2) the variant isoforms of CD44 (CD44v). CD44s is encoded by ten constant exons. CD44v is encoded by ten constant exons and any combination of the remaining nine exons (Prochazka et al., 2014). Different isoforms of CD44 possess similar or distinct cellular functions (Chen et al., 2018).

Compared with normal tissues, CD44 is overexpressed in a variety of tumors, including glioma (Dosio et al., 2016). Some studies have reported that increased expression levels of CD44 are associated with a poor prognosis in Glioblastoma patients (Anido et al., 2010; Bhat et al., 2013; Jijiwa et al., 2011; Nishikawa et al., 2018; Pietras et al., 2014; Wang et al., 2018), while others found no correlation (Ranuncolo et al., 2002; Tsidulko et al., 2017). Still, others have identified CD44 as a positive prognostic indicator of survival for GBM patients (Wei et al., 2010). Klank et al., suggested a biphasic relationship between *CD44* expression levels and survival of glioma patients (Klank et al., 2017).

GSCs define a small subpopulation of tumor cells in GBM with the ability to self-renew, and to differentiate into tumor lineages and initiate tumors. GSCs in GBM are responsible for tumor progression, chemo-resistance, radio-resistance, recurrence, and metastasis (Galli et al., 2004; Singh et al., 2004). CD44 is recognized as a cancer stem cell marker in various cancers (Yan et al., 2015); however, whether or not CD44 is an applicable GSC marker remains controversial. Several studies support the suggestion that CD44 might be a GSC marker(Brown et al., 2015; Brown et al., 2017; Tanaka et al., 2015). However, Wang et al., have found that CD44 low-expressing cells exhibit more GSC traits, and his group suggested that CD44 is not an appropriate GSC marker (Wang et al., 2017).

Compared to GBM, the prognostic value of *CD44* for grade II/III glioma patients has not been investigated. In the present study, we investigated in the gene expression patterns of total *CD44*, *CD44s*, and *CD44v2–v10* in grade II/III gliomas. We correlated gene expression of *CD44* to the clinical characteristics of glioma patients, and estimated its potential prognostic value for grade II/III glioma patients. Moreover, a gene set enrichment analysis (GSEA) was performed to explore the function of *CD44* and its related signaling pathways.

Methods and Materials

Oncomine analysis

To evaluate the mRNA expression of *CD44* in glioma tissues as compared to normal tissues,

previously published and publicly available microarray data in the online Oncomine database (www.oncomine.com; Oncomine™, Compendia Bioscience, Ann Arbor, MI, USA) was used. RNA expression levels are reported as Log_2 median-centered intensity in the Oncomine database. *CD44* mRNA expression levels in tumor specimens were compared with that in normal controls by the Student's t-test to generate a P value.

Patients in Hokkaido University Hospital

A cohort of 112 patients from the department of Neurosurgery in Hokkaido University Hospital (HUH) between January 2003 and March 2019 were evaluated. All the patients were diagnosed as grade II or III gliomas based on WHO 2000 criteria, WHO 2007 criteria, or WHO 2016 criteria. Patient who was younger than 16 years old at the time of diagnosis was excluded from the present study. Both clinical data and detailed follow-up data were obtained for all patients. The isocitrate dehydrogenase (IDH) mutation status was investigated using Sanger sequencing. In addition, we also investigated in the 1p/19q loss of heterozygosity status of the tumors using a multiplex ligation-dependent probe amplification procedure. The present study was approved by the local Ethics Committee at Hokkaido University Hospital (Sapporo, Japan; 015-0154). As this study was retrospective, informed consent was waived by the IRB. All procedures performed in the present study were in accordance with 1964 Helsinki Declaration and its later amendments.

RNA extraction and Quantitative real-time polymerase chain reaction (qPCR) analysis

The total RNA was extracted from the frozen specimens stored in -80˚C using a RNeasy Mini Kit (QIAGEN, Hilden, Germany). cDNA was synthesized using the PrimeScript™ II 1st Strand cDNA Synthesis kit (Takara Biotechnology Co., Ltd., Dalian, China) with 1 mg of total RNA. The primer sequences of *CD44*, *CD44s*, *CD44v2*, *CD44v3*, *CD44v4*, *CD44v5*, *CD44v6*, *CD44v7*, *CD44v8*, *CD44v9*, *CD44v10*, and *β-actin* are listed in Table 1. Reverse transcription-qPCR analysis was performed using FastStart Essential DNA Green Master with LightCycler 96 (Roche Diagnostics, Basel, Switzerland). The PCR product specificities were confirmed by melt curve analysis. All PCR experiments were done in triplicates, and the means of three values are presented. The relative target gene mRNA expression levels

compared to β-actin were measured by qPCR using the $2^{-\Delta\Delta CT}$ method (Livak and Schmittgen, 2001).

Table 1. The primer sequences of *CD44, CD44s, CD44v2, CD44v3, CD44v4, CD44v5, CD44v6, CD44v7, CD44v8, CD44v9, CD44v10*, and *β-actin.*

Gene	Forward Primer (5'-3')	Reverse Primer (5'-3')
CD44	GATGGAGAAAGCTCTGAGCATC	TTGCTGCACAGATGGAGTTG
CD44s	GGAGCAGCACTTCAGGAGGTTAC	GGAATGTGTCTTGGTCTCTGGTAGC
CD44v2	ATCACCGACAGCACAGACAGAAT	AACCATGAAAACCAATCCCAGG
CD44v3	TACGTCTTCAAATACCATCTCAGCA	AATCTTCATCATCATCAATGCCTG
CD44v4	AACCACACCACGGGCTTTTG	TCCTTGTGGTTGTCTGAAGTAGCA
CD44v5	TGCTTATGAAGGAAACTGGAAC	TGTGCTTGTAGAATGTGGGGT
CD44v6	CCAGGCAACTCCTAGTAGTACAACG	CGAATGGGAGTCTTCTTTGGGT
CD44v7	GCCTCAGCTCATACCAGCCATC	TCCTTCTTCCTGCTTGATGACCT
CD44v8	TGGACTCCAGTCATAGTATAACGC	GGTCCTGTCCTGTCCAAATC
CD44v9	AGCAGAGTAATTCTCAGAGC	TGATGTCAGAGTAGAAGTTGTT
CD44v10	CCTCTCATTACCCACACACG	CAGTAACTCCAAAGGACCCA
β-actin	GTGAAGGTGACAGCAGTCGGTT	GAAGTGGGGTGGCTTTTAGGAT

Data mining in TCGA and CGGA

Clinical information, gene expression, and gene mutation status were obtained from the Cancer Genome Atlas (TCGA, https://portal.gdc.cancer.gov/) database and the Chinese Glioma Genome Atlas (CGGA, http://cgga.org.cn/) database for grade II/III glioma patients. Patient who was less than 16 years old at the time of diagnosis was excluded. Patients without survival data were also excluded from the present study. The raw count data of RNA-seq was obtained from TCGA and then normalized using the edgeR package (version 3.26.1) in R (version 3.5.3). The RNA-seq data from the CGGA database was presented directly as the value of fragments per kilobase per million mapped reads (FPKM).

Gene set enrichment analysis

GSEA is a method to identify groups of genes or proteins that are over-represented in a large set of genes or proteins. These groups of genes or proteins may have an association with biological functions or phenotypes. In the present study, the phenotype was determined by the expression level of *CD44* (high versus low) based on the TCGA database. We selected annotated gene sets (c2.cp.kegg. v6.2 symbols) as the reference gene sets. The normalized enrichment score (NES), nominal p-value, and false discovery rate (FDR) q-value were used to indicate the significance of association between the gene sets and the pathways.

Statistical analysis

The mRNA expression levels of *CD44* were compared by the Mann-Whitney U-test between groups. Categorical variables were expressed as frequency and were compared using the Chi-square ($\chi 2$) test. The value of *CD44* mRNA expression higher than the median value was considered as *CD44* high expression, while the value of *CD44* mRNA expression level lower than the median value was considered as *CD44* low expression. OS and PFS were presented as Kaplan-Meier curves. The Kaplan-Meier survival curves with the log-rank test were calculated and then plotted using Graphpad Prism version 8. Univariate and multivariate Cox proportional hazard regression analyses were conducted using SPSS version 22.0. Factors that were significant at the 0.1 level on univariate analysis were selected for multivariate analysis. $P < 0.05$ was considered to indicate a statistically significant difference.

Results

The mRNA expression levels of CD44 in glioma tissues and normal brain tissues

Based on the data in the Oncomine database, we further confirmed that *CD44* mRNA expression was significantly higher in glioma tissues as compared to normal brain tissues (Fig. 1 and 2).

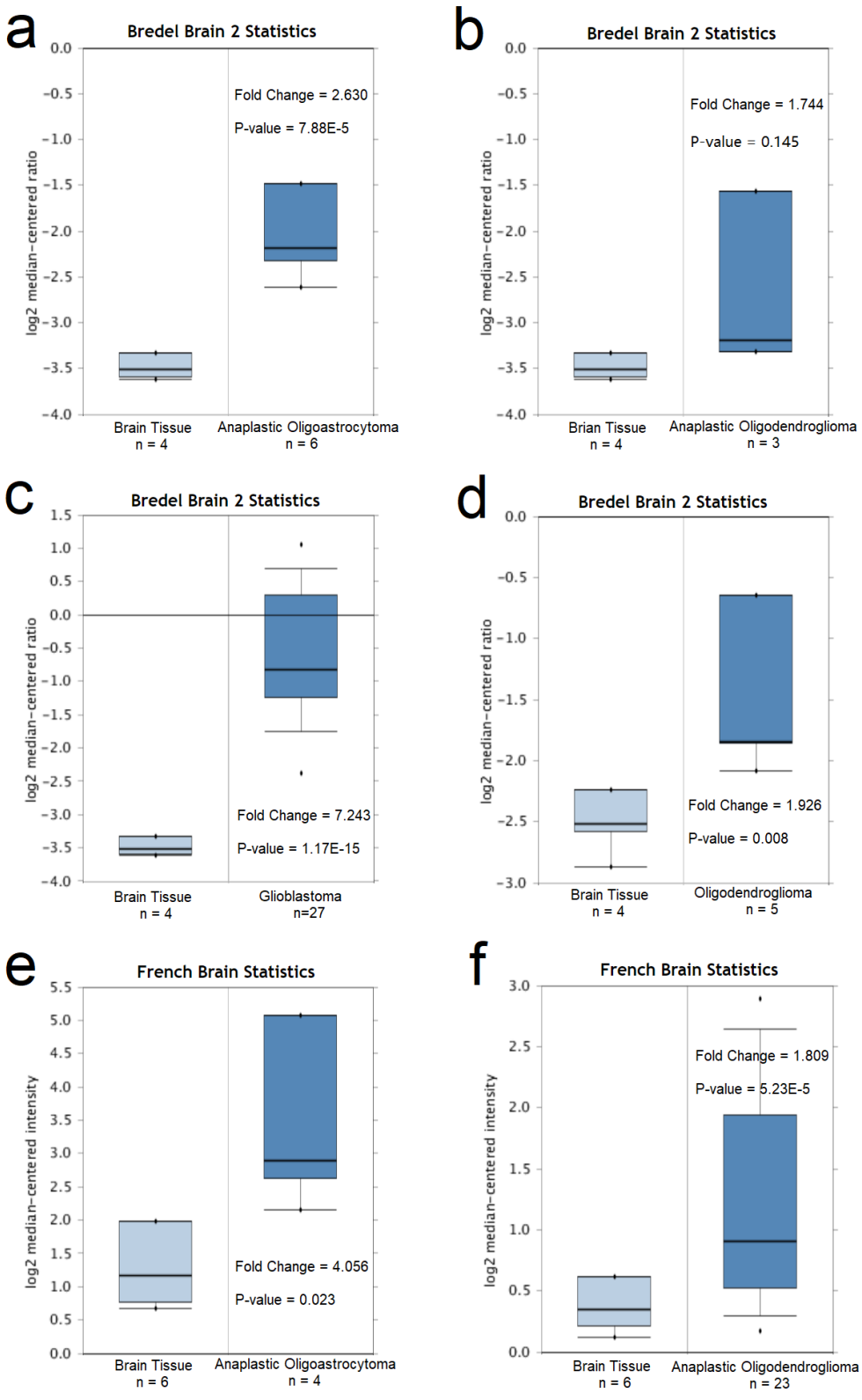

Figure 1. Oncomine microarray database was used to evaluate the mRNA expression of CD44 in glioma tissues vs. normal brain tissues. **a to d** Box plots derived from gene expression data of Bredel study. **e and f** Box plots derived from gene expression data of French study. RNA expression levels are reported as Log2 median-centered intensity. CD44 mRNA expression levels in tumor specimens were compared with that in normal controls by the Student's t-test to generate a P value.

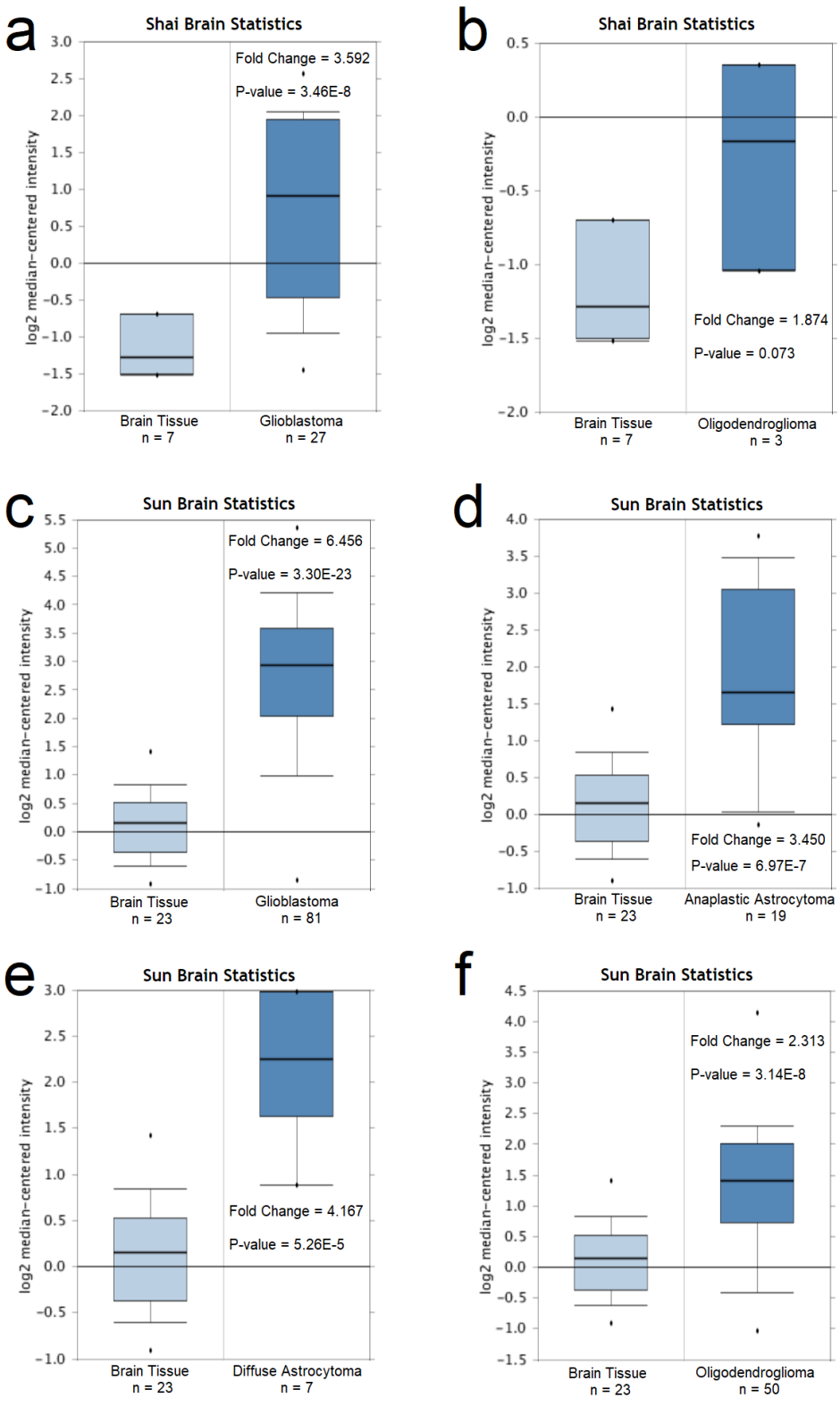

Figure 2. Oncomine microarray database was used to evaluate the mRNA expression of CD44 in glioma tissues vs. normal brain tissues. **a and b** Box plots derived from gene expression data of Shai study. **c to f** Box plots derived from gene expression data of Sun study. RNA expression levels are reported as Log2 median-centered intensity. CD44 mRNA expression levels in tumor specimens were compared with that in normal controls by the Student's t-test to generate a P value.

The mRNA expression levels of CD44, CD44s, CD44v2, CD44v3, CD44v4, CD44v5, CD44v6, CD44v7, CD44v8, CD44v9, and CD44v10 in grade II/III gliomas

Compared with mRNA expression level of CD44s, the mRNA expression levels of *CD44v3, CD44v4, CD44v5, CD44v6, CD44v7, CD44v8, CD44v9,* and *CD44v10* were much lower (Fig. 3). Further, extremely low mRNA expression level of CD44v2 was detected in grade II/III gliomas. We even failed to detect the mRNA expression of *CD44v2* in 30 specimens. Besides, tumor specimens which belonged to *CD44* high group also belonged to *CD44s* high group (data not shown). Thus, in grade II/III gliomas, the mRNA expression level of *CD44s* could practically represent the mRNA expression level of total *CD44*.

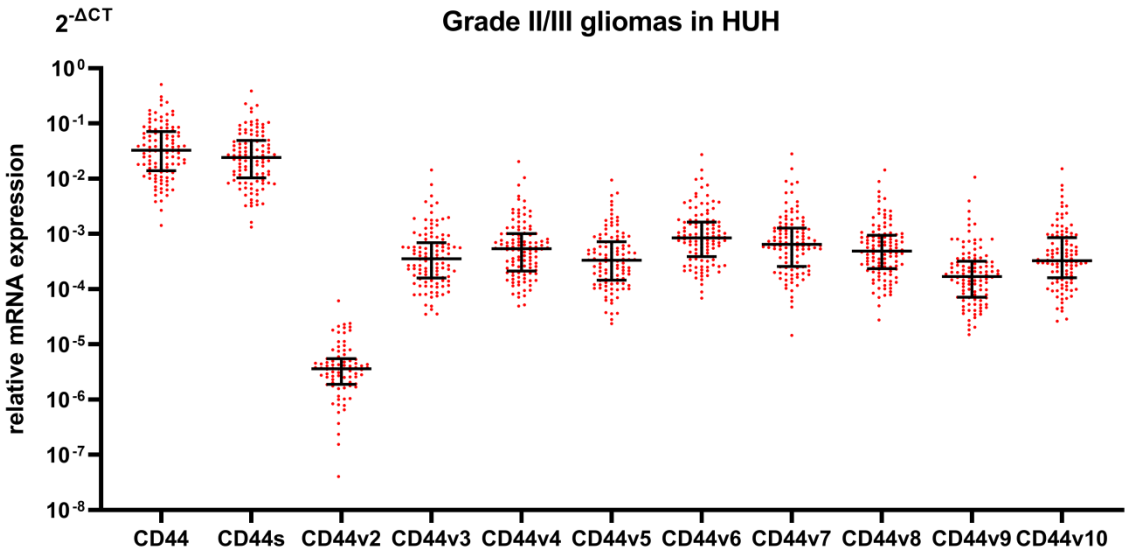

Figure 3. The mRNA expression levels of CD44, CD44s, and CD44v2–v10 in grade II/III gliomas in the HUH cohorts.

The relationship between the mRNA expression levels of CD44 and the clinicopathological characteristics seen in glioma patients

Based on the RNA-seq data in the TCGA and CGGA databases, and the qPCR analysis of the glioma cases in HUH, we next explored the relationship between *CD44* mRNA expression levels and various clinicopathological characteristics seen in grade II/III glioma patients (Table 2, 3 and 4, Fig. 4). In HUH cohorts, compared with patients younger than 60 years old, *CD44* expression was significantly higher in patients over 60 years old (Fig. 4a). The *CD44*

expression levels in IDH wild type tumors were significantly higher than that in IDH mutant tumors (Fig. 4g). In the TCGA cohorts, the *CD44* expression levels in grade III gliomas and IDH wild type gliomas were significantly higher than that in grade II gliomas and IDH mutant gliomas, respectively (Fig. 4e, h). Besides, high *CD44* expression level was significantly associated with high recurrent probability (Fig. 4m). In the CGGA cohorts, the *CD44* expression levels in 1p/19q non co-deleted gliomas were significantly higher than that in 1p/19q co-deleted gliomas (Fig. 2k).

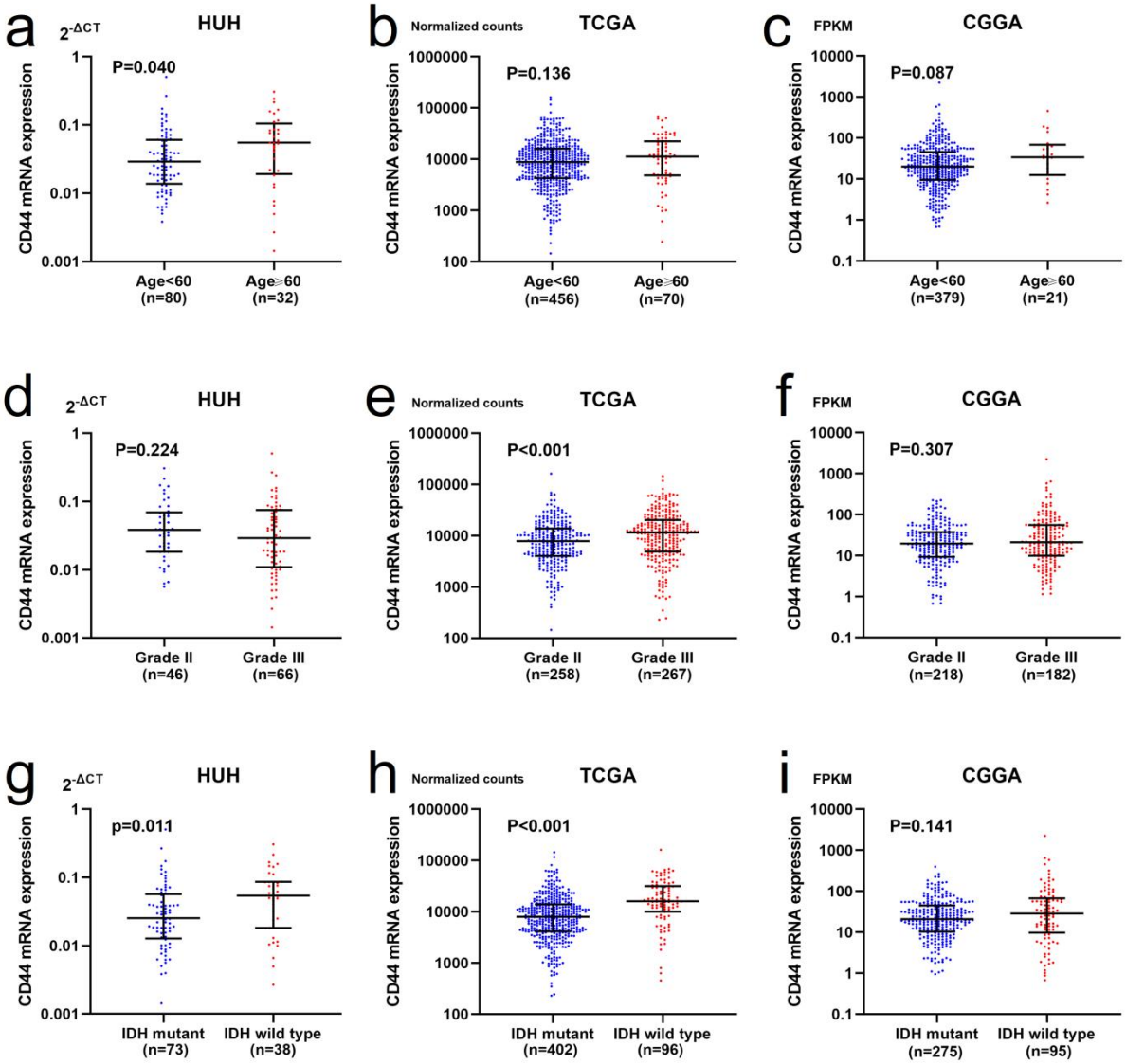

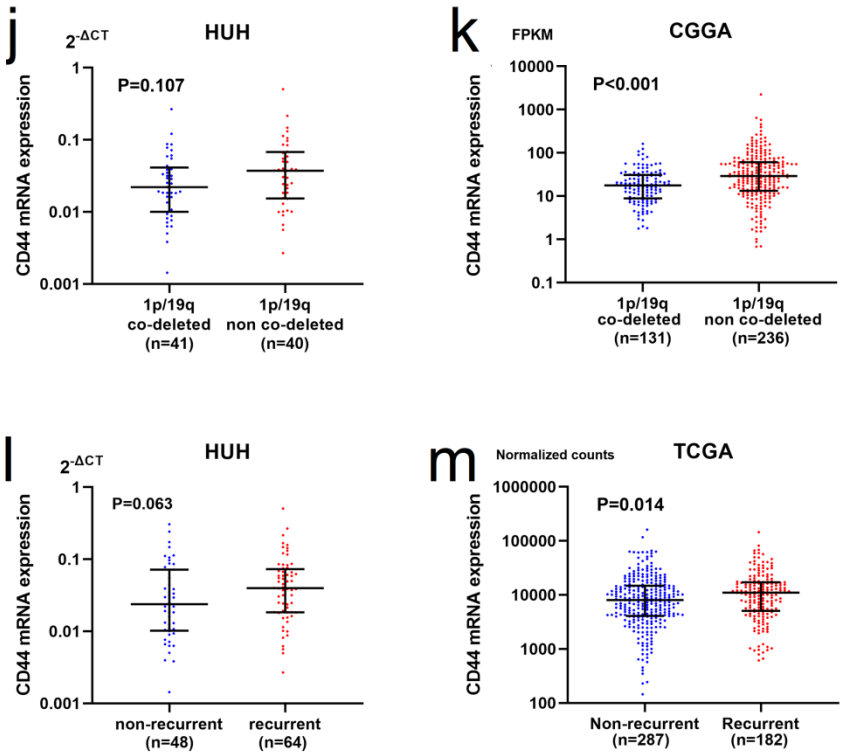

Figure 4. The relationship between *CD44* mRNA expression levels and the clinicopathological characteristics in the HUH cohorts, the TCGA cohorts, and the CGGA cohorts. Data are presented as median with the first and third quartiles: **a to c** age < 60 years old and age ≥ 60 years old; **d to f** grade of gliomas; **g to i** IDH status of gliomas; **j and k** 1p/19q status of gliomas; **l and m** recurrent status.

Table 2. Patient characteristics and the relationship between CD44 mRNA expression and clinicopathological characteristics in grade II/III gliomas in Hokkaido University Hospital cohorts.

Parameters	**No. of patients(%)**	**Total CD 44 expression**		**P value**
		High (n=56)	**Low (n=56)**	
Age (years)				0.020
<60	81	35	46	
≥60	31	21	10	
Gender				0.449
Male	58	27	31	
Female	54	29	25	
Grade				0.249
II	46	26	20	
III	66	30	36	
KPS				0.675
≥70	106	52	54	
<70	6	4	2	

IDH status				0.014
IDH wild type	38	25	13	
IDH mutant	73	30	43	
Unknown	1	1	0	
1p/19q status				0.095
1p/19q co-deleted	41	14	27	
1p/19q non co-deleted	40	21	19	
Unknown	31	21	10	
Surgery				0.522
Biopsy	18	9	9	
Partial resection	67	36	31	
Total resection	27	11	16	
Adjuvant chemotherapy				0.321
Yes	73	34	39	
No	39	22	17	
Adjuvant radiotherapy				1.000
Yes	70	35	35	
No	42	21	21	
Recurrence status				0.056
Yes	64	37	27	
No	48	19	29	

KPS, Karnofsky performance score; IDH, isocitrate dehydrogenase.

Table 3. Patient characteristics and the relationship between CD44 mRNA expression and clinicopathological characteristics in grade II/III glioma patients based on the TCGA database.

Parameters	**No. of patients(%)**	**CD 44 expression**		**P value**
		High (n=263)	**Low (n=263)**	
Age (years)				0.072
<60	456	221	235	
≥60	70	42	28	
Gender				0.381
Male	288	149	139	
Female	238	114	124	
Grade				0.001
II	258	110	148	
III	267	152	115	
Unknown	1	1	0	
KPS				0.637
≥70	289	144	145	
<70	18	10	8	
Unknown	219	109	110	
IDH status				<0.001
IDH wild type	96	73	23	
IDH mutant	402	177	225	

Unknown	28	13	15	
Adjuvant radiotherapy				0.001
Yes	305	171	134	
No	97	35	62	
Unknown	124	57	67	
Adjuvant chemotherapy				0.148
Yes	269	136	133	
No	102	43	59	
Unknown	155	84	71	
Recurrence status				0.008
Yes	182	104	78	
No	287	128	159	
Unknown	57	31	26	

KPS, Karnofsky performance score; IDH, isocitrate dehydrogenase.

Table 4. Patient characteristics and the relationship between CD44 mRNA expression and clinicopathological characteristics in grade II/III glioma patients based on the CGGA database.

Parameters	**No. of patients(%)**	**CD 44 expression**		**P value**
		High (n=200)	**Low (n=200)**	
Age (years)				0.117
<60	379	186	193	
≥60	21	14	7	
Gender				0.187
Male	233	123	110	
Female	167	77	90	
Grade				0.688
II	218	107	111	
III	182	93	89	
IDH status				0.240
IDH wild type	95	55	40	
IDH mutant	275	140	135	
Unknown	30	5	25	
1p/19q status				<0.001
1p/19q co-deleted	131	52	79	
1p/19q non co-deleted	236	146	90	
Unknown	33	2	31	
Adjuvant radiotherapy				0.147
Yes	325	167	158	
No	65	27	38	
Unknown	10	6	4	
Adjuvant chemotherapy				0.965
Yes	230	113	117	
No	156	77	79	

Unknown	14	10	4

IDH, isocitrate dehydrogenase.

To some extent, the majority of the results showed the similar tendency among the HUH cohorts, the TCGA cohorts, and the CGGA cohorts, although some of the results did not reach statistical significance. The above results indicated that *CD44* expression was associated with various clinicopathological characteristics and might serve as a potential prognostic biomarker for glioma patients.

The correlation between CD44 expression and overall survival of glioma patients

The Kaplan-Meier survival curves and log-rank test analyses illustrated that high expression of *CD44* was significantly associated with poor OS of grade II/III gliomas in the HUH cohorts, the TCGA cohorts and the CGGA cohorts (Fig. 5).

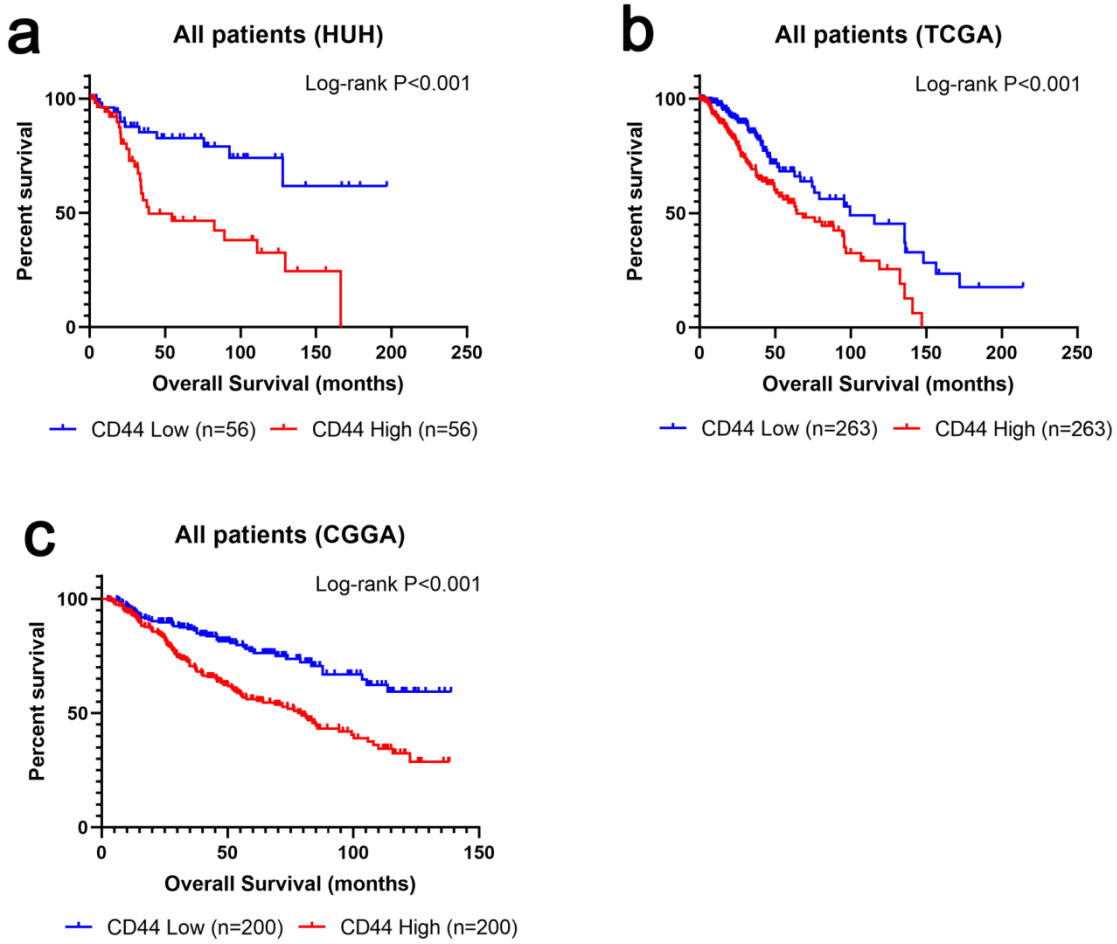

Figure 5. Correlation between *CD44* mRNA expression and OS of glioma patients. **a** The association between *CD44* mRNA expression and OS in all grade II/III glioma patients in HUH cohorts. **b** The association between

CD44 mRNA expression and OS in all grade II/III glioma patients in the TCGA cohorts. **c** The association between *CD44* mRNA expression and OS in all grade II/III glioma patients in the CGGA cohorts.

The correlation between CD44 expression and progression-free survival of glioma patients

The results of the survival analyses demonstrated that high *CD44* mRNA expression was significantly associated with a poor PFS of grade II/III glioma patients (Fig. 6a). Moreover, high CD44 expression was significantly associated with a poor PFS of each subgroup (Fig. 6b to e).

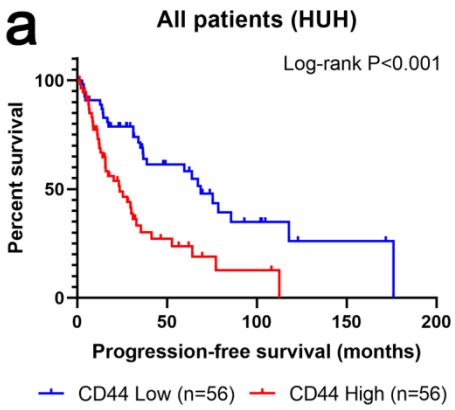

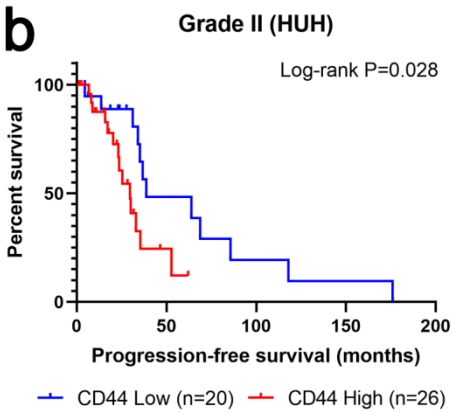

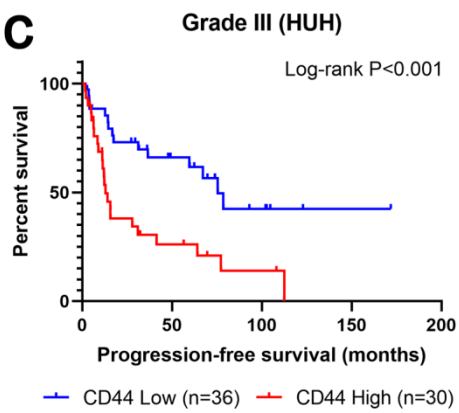

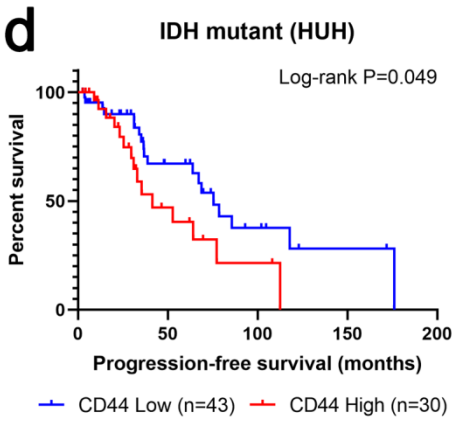

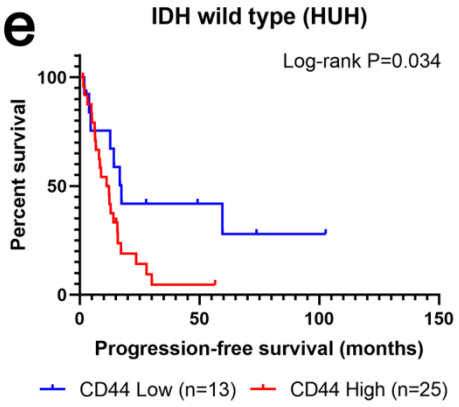

Figure 6. Correlation between *CD44* mRNA expression and PFS of glioma patients. **a** The association between *CD44* mRNA expression and PFS in all grade II/III glioma patients in HUH cohorts. **b** The association between *CD44* mRNA expression and PFS in grade II gliomas. **c** The association between *CD44* mRNA expression and PFS in grade III gliomas. **d** The association between *CD44* mRNA expression and PFS in IDH mutant gliomas. **e** The association between *CD44* mRNA expression and PFS in IDH wild type gliomas.

Subgroup analysis of the correlation between CD44 expression and overall survival of glioma patients

We then performed survival analysis towards *CD44* mRNA expression in subgroups of grade II/III gliomas (Fig. 7). The results suggested a similar tendency that high *CD44* expression was associated with a poor OS of each subgroup, although inconsistencies exist among the three cohorts. Thus, we suggest that *CD44* could serve as a potential prognostic factor for grade II/III glioma patients.

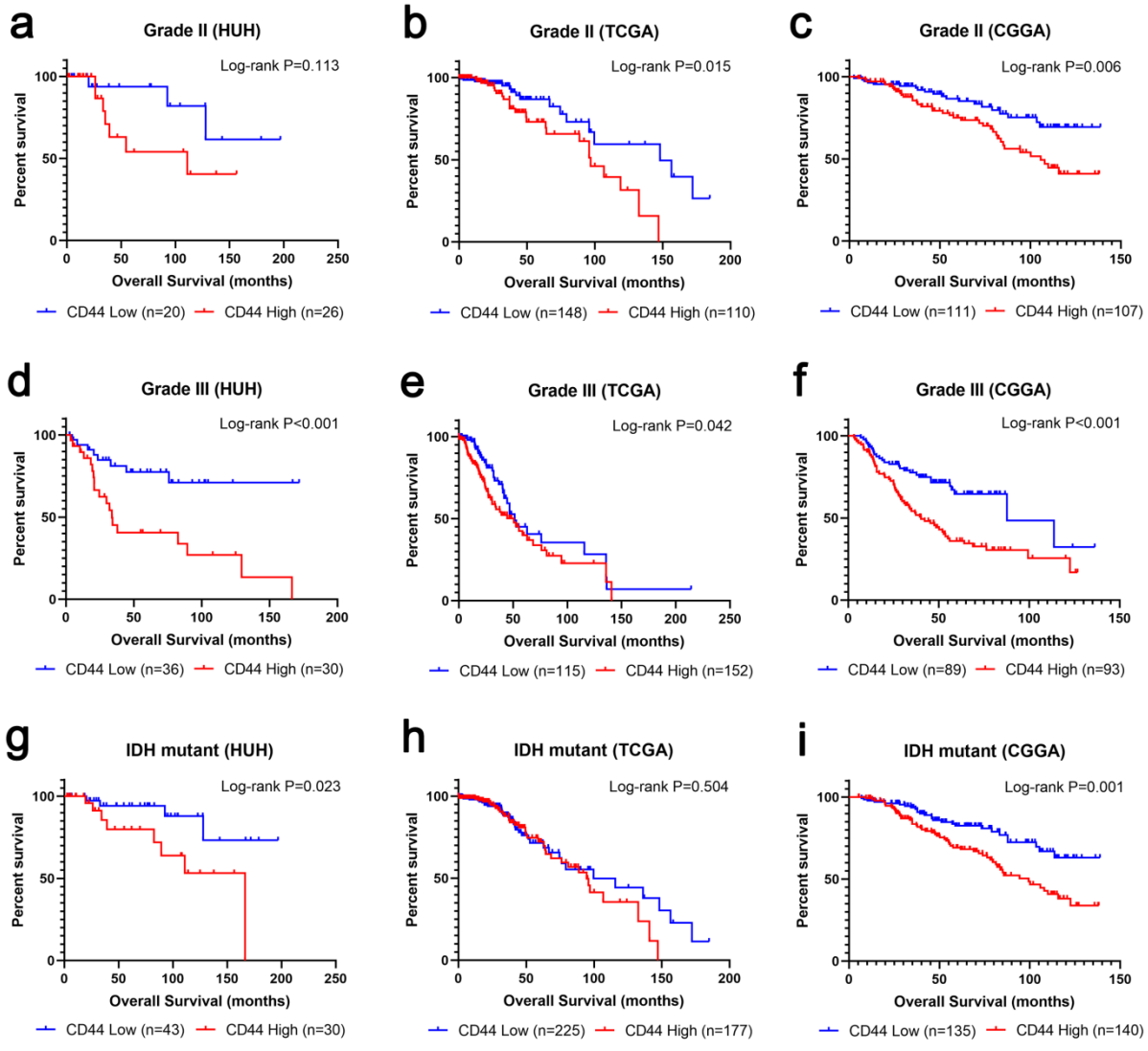

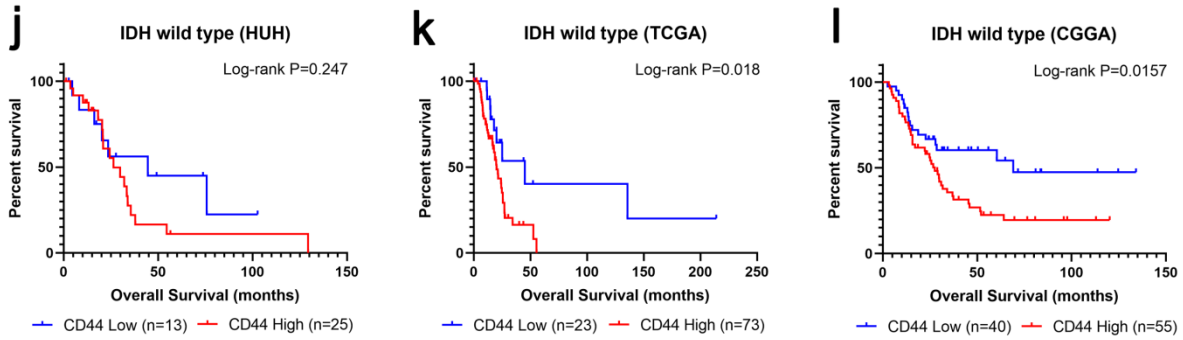

Figure 7. The correlation between *CD44* mRNA expression and OS of glioma patients. **a to c** The association between *CD44* mRNA expression and OS in grade II gliomas. **d to f** The association between *CD44* mRNA expression and OS in grade III gliomas. **g to i** The association between *CD44* mRNA expression and OS in IDH mutant gliomas. **j to l** The association between *CD44* mRNA expression and OS in IDH wild type gliomas.

CD44 was an independent prognostic marker for grade II/III glioma patients

Based on the above findings, we used univariate and multivariate Cox regression analyses to evaluate the utility of *CD44* expression as an independent prognostic factor (Table 5, 6 and 7). Multivariate Cox regression analyses found that *CD44* expression was significantly associated with OS as a prognostic factor in the HUH cohorts (P = 0.027), the TCGA cohorts (P = 0.029), and the CGGA cohorts (P = 0.003).

Table 5. Univariate and multivariate Cox proportional hazard regression analyses of overall survival in grade II/III gliomas in Hokkaido University Hospital cohorts.

Variables	**Univariate cox regression**		**Multivariate cox regression**	
	HR (95% CI)	**P value**	**HR (95% CI)**	**P value**
Age				
<60	Reference		Reference	
≥60	3.595 (1.855-6.967)	<0.001	0.680 (0.261-1.775)	0.431
Grade				
II	Reference		Reference	
III	1.986 (0.957-4.123)	0.065	1.188 (0.519-2.721)	0.684
KPS				
≥70	Reference		Reference	
<70	2.636 (0.924-7.522)	0.070	0.638 (0.200-2.032)	0.447
IDH status				
IDH wild type	Reference		Reference	
IDH mutant	0.102 (0.049-0.214)	<0.001	0.131 (0.053-0.322)	<0.001
Surgery				
Biopsy	Reference		Reference	

Partial resection	0.107 (0.048-0.241)	<0.001	0.143 (0.055-0.372)	<0.001
Total resection	0.122 (0.047-0.317)	<0.001	0.164 (0.054-0.500)	0.001
CD44 expression				
Low	Reference		Reference	
High	3.344 (1.643-6.807)	0.001	2.632 (1.115-6.216)	0.027

KPS, Karnofsky performance score; IDH, isocitrate dehydrogenase; HR, hazard ration; CI, conficence interval.

Table 6. Univariate and multivariate Cox proportional hazard regression analyses of overall survival in grade II/III gliomas base on the TCGA database.

Variables	**Univariate cox regression**		**Multivariate cox regression**	
	HR (95% CI)	**P value**	**HR (95% CI)**	**P value**
Age				
<60	Reference		Reference	
≥60	4.917 (3.248-7.443)	<0.001	3.097 (1.988-4.826)	<0.001
Grade				
II	Reference		Reference	
III	3.188 (2.203-4.612)	<0.001	2.168 (1.473-3.191)	<0.001
KPS				
≥70	Reference		Reference	
<70	4.644 (2.219-9.720)	<0.001	2.336 (1.101-4.957)	0.027
Unknown	0.816 (0.560-1.188)	0.288	0.785 (0.536-1.149)	0.212
IDH status				
IDH wild type	Reference		Reference	
IDH mutant	0.158 (0.109-0.230)	<0.001	0.260 (0.174-0.390)	<0.001
Unknown	0.203 (0.109-0.378)	<0.001	0.352 (0.182-0.682)	0.002
CD44 expression				
Low	Reference		Reference	
High	1.960 (1.370-2.804)	<0.001	1.516 (1.043-2.202)	0.029

KPS, Karnofsky performance score; IDH, isocitrate dehydrogenase; HR, hazard ration; CI, conficence interval.

Table 7. Univariate and multivariate Cox proportional hazard regression analyses of overall survival in grade II/III gliomas base on the CGGA database.

Variable	**Univariate cox regression**		**Multivariate cox regression**	
	HR (95% CI)	**P value**	**HR (95% CI)**	**P value**
Age				
<60	Reference		Reference	
≥60	3.302 (1.930-5.650)	<0.001	1.992 (1.132-3.505)	0.017
Grade				
II	Reference		Reference	
III	2.725 (1.939-3.829)	<0.001	2.283 (1.615-3.228)	<0.001
IDH status				
IDH wild type	Reference		Reference	

IDH mutant	0.266 (0.189-0.374)	<0.001	0.509 (0.353-0.733)	<0.001
Unknown	0.193 (0.077-0.482)	<0.001	0.440 (0.171-1.132)	0.089
1p/19q status				
1p/19q non co-deleted	Reference		Reference	
1p/19q co-deleted	0.152 (0.090-0.258)	<0.001	0.212 (0.122-0.367)	<0.001
Unknown	0.688 (0.371-1.277)	0.236	0.890 (0.457-1.733)	0.732
CD44 expression				
Low	Reference		Reference	
High	2.203 (1.560-3.112)	<0.001	1.780 (1.218-2.602)	0.003

IDH, isocitrate dehydrogenase; HR, hazard ration; CI, conficence interval.

Gene set enrichment analysis

We performed GSEA to explore the function of *CD44* and its related signaling pathways base on the TCGA database. The significantly enriched signaling pathways were picked out according to the NES, FDR q-value, and nominal p-value. In the present study, gene sets of Toll-like receptors (TLRs) signaling pathway, cell adhesion molecules, regulation of actin cytoskeleton, and chemokine signaling pathway are differentially enriched in *CD44* high expression phenotype (Table 8, Fig. 8).

Table 8. Gene sets enrichment in CD44 high expression phenotype

Gene set name	**NES**	**Nominal p-value**	**FDR q-value**
KEGG_TOLL_LIKE_RECEPTOR_SIGNALING_PATHWAY	2.06371	<0.001	0.002
KEGG_CELL_ADHESION_MOLECULES_CAMS	2.06173	<0.001	0.002
KEGG_REGULATION_OF_ACTIN_CYTOSKELETON	1.87839	<0.001	0.015
KEGG_CHEMOKINE_SIGNALING_PATHWAY	1.82030	0.008	0.020

NES, normalized enrichment score; FDR, false discovery rate.

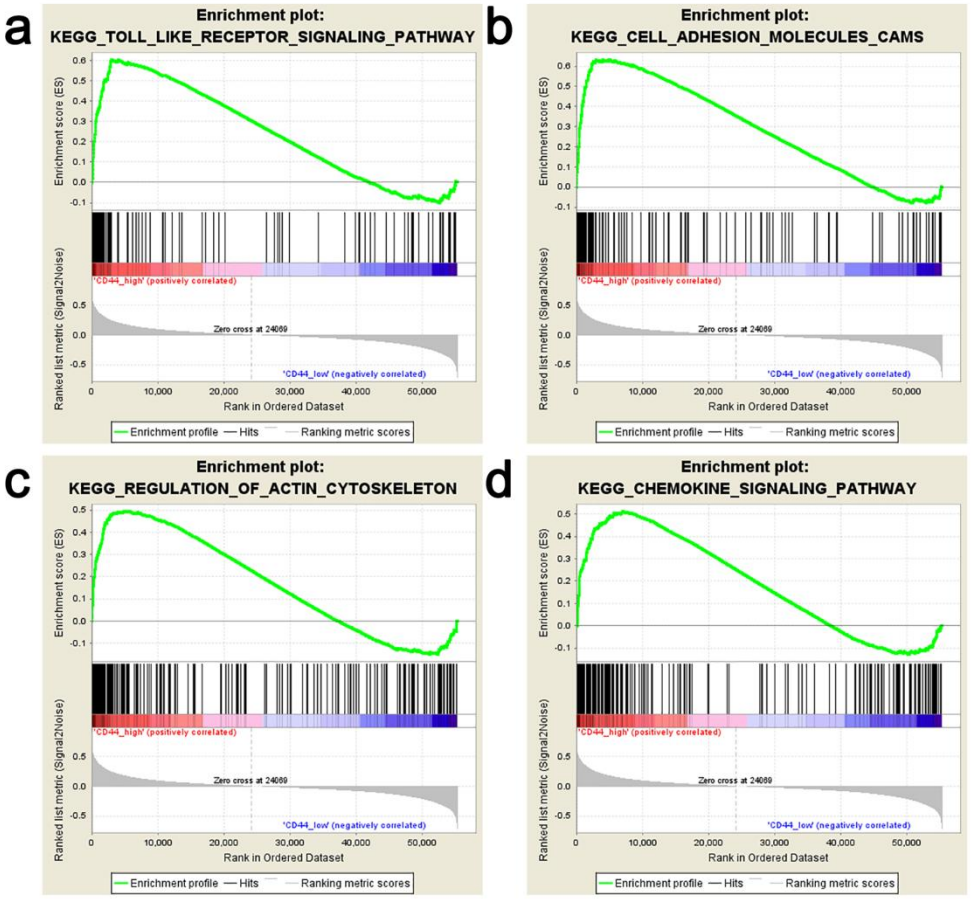
a
Enrichment plot:
KEGG_TOLL_LIKE_RECEPTOR_SIGNALING_PATHWAY
b
Enrichment plot:
KEGG_CELL_ADHESION_MOLECULES_CAMS
c
Enrichment plot:
KEGG_REGULATION_OF_ACTIN_CYTOSKELETON
d
Enrichment plot:
KEGG_CHEMOKINE_SIGNALING_PATHWAY
Enrichment score (ES)
Ranked list metric (Signal2Noise)
'CD44_high' (positively correlated)
Zero cross at 24089
'CD44_low' (negatively correlated)
Rank in Ordered Dataset
Enrichment profile
Hits
Ranking metric scores

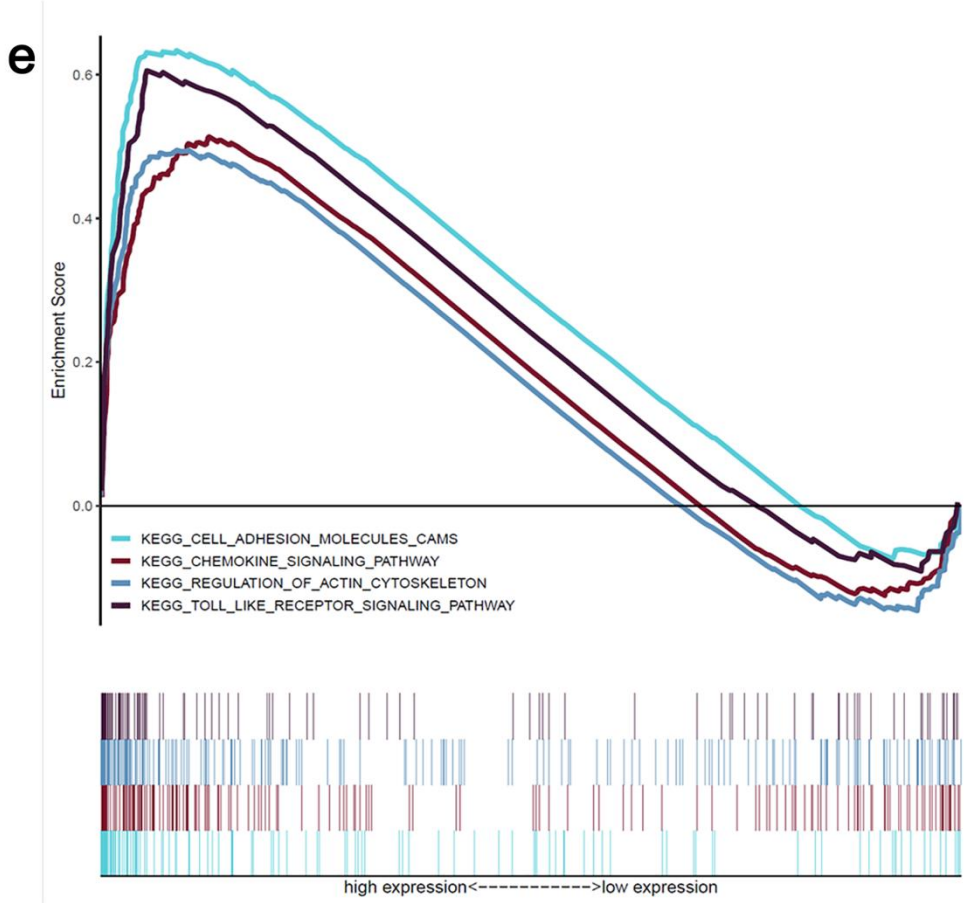
e
Enrichment Score
KEGG_CELL_ADHESION_MOLECULES_CAMS
KEGG_CHEMOKINE_SIGNALING_PATHWAY
KEGG_REGULATION_OF_ACTIN_CYTOSKELETON
KEGG_TOLL_LIKE_RECEPTOR_SIGNALING_PATHWAY
high expression<----------->low expression

Figure 8. Enrichment plots from Gene Set Enrichment Analysis. **a** Toll-like receptor signaling pathway enriched in *CD44* high expression phenotype. **b** Cell adhesion molecules enriched in *CD44* high expression phenotype. **c** Gene set of regulation of actin cytoskeleton enriched in *CD44* high expression phenotype. **d** Chemokine signaling pathway enriched in *CD44* high expression phenotype. **e** A merged plot showing the pathways mentioned above.

Discussion

Overexpression of HA is correlated with poor prognosis in many cancer types (Tammi et al., 2008). CD44, which is a major cell surface receptor for HA and many other extracellular matrix components, is implicated in cell adhesion, migration, and signaling (Ponta et al., 2003).

There are two families of CD44 isoforms: 1) the standard isoform of CD44; and 2) the variant isoforms of CD44 (Chen et al., 2018). Miwa et al., found that CD44s cells were associated with increased chemotaxis, invasiveness, and decreased tumorigenicity in gallbladder cancer, while CD44v cells were associated with decreased chemotaxis, invasiveness, and increased tumorigenicity (Miwa et al., 2017). In human gliomas, Ranuncolo et al., found that overexpression of CD44s is associated with a highly invasive behavior (Ranuncolo et al., 2002). CD44s appears to be the dominant form of CD44 in primary brain tumors (Ariza et al., 1995; Kaaijk et al., 1995). Expression levels of CD44s do not seem to correlate with the grading range of gliomas (Kaaijk et al., 1995; Ylagan and Quinn, 1997). Several studies have demonstrated that absent or low expression of CD44v was found in primary brain tumors, although high expression levels of CD44v were detected in metastatic brain tumors (Ariza et al., 1995; Li et al., 1993; Li et al., 1995; Ranuncolo et al., 2002; Resnick et al., 1999). Thus, the lack of CD44v expression might be one of the explanations for the lack of metastatic potential of gliomas. In other words, CD44v might play a role in the intracranial spread of metastatic brain tumors. However, Kaaijk et al. suggest a strong focal expression of CD44v5 in highly malignant gliomas (Kaaijk et al., 1995).

GSCs are considered to be largely responsible for the poor prognosis of GBMs (Auffinger et al., 2015); however, whether or not CD44 could be a useful GSC marker remains

controversial, although it has been considered as a cancer stem cell marker for many types of tumors (Brown et al., 2015; Brown et al., 2017; Tanaka et al., 2015; Wang et al., 2017; Yan et al., 2015). Several studies have explored the prognostic significance of CD44 for GBM patients, but the results are inconsistent (Anido et al., 2010; Bhat et al., 2013; Jijiwa et al., 2011; Klank et al., 2017; Nishikawa et al., 2018; Pietras et al., 2014; Ranuncolo et al., 2002; Tsidulko et al., 2017; Wang et al., 2018; Wei et al., 2010). Moreover, the prognostic value of CD44 for grade II/III glioma patients has not been studied.

In the present study, we confirmed that *CD44* expression was significantly up-regulated in glioma tissues. Further, we confirmed that *CD44s* is the dominant form of *CD44* in grade II/III gliomas. *CD44* expression was associated with the age of patients, IDH status, tumor WHO grade, and recurrent probability of grade II/III gliomas. We then performed survival analyses. The Kaplan-Meier survival curve analysis and log-rank test revealed that high *CD44* expression was significantly associated with poor OS and PFS in grade II/III glioma patients, which suggested that *CD44* mRNA expression might serve as a prognostic factor for grade II/III gliomas. Multivariate cox regression analyses further confirmed that *CD44* expression might serve as an independent prognostic factor for grade II/III glioma patients. Next, we found that gene sets of Toll-like receptors (TLRs) signaling pathway, cell adhesion molecules, regulation of actin cytoskeleton, and chemokine signaling pathway are differentially enriched in *CD44* high expression phenotype.

Toll like receptor signaling pathway

TLRs are expressed by various immune cells, endothelial cells, epithelial cells, and tumor cells. Modulation of TLR signaling can have anti- and pro-tumor effects depending on the TLR, the tumor subtype, and the immune cells infiltrating the tumor. The pro-tumor effect is mainly driven by TLR expressed by tumor cells (Dajon et al., 2017). The stimulation of TLR in tumor cells could result in increased cell survival and proliferation, or resistance to chemotherapy (Dajon et al., 2017). It has been reported that high expression TLR2 and TLR9 is associated with poor prognosis of glioma patients. The contribution of TLR2, TLR4, and TLR9 to glioma progression has been mostly described as tumor promoting (Jiang et al.,

2018; Li et al., 2019; Wang et al., 2010). Qadri et al. suggested that TLR2 activation could be regulated by CD44 (Qadri et al., 2018).

Regulation of actin cytoskeleton

The actin cytoskeleton is essential for whole cell migration and cell interaction with the environment (Svitkina, 2018). Infiltration of glioma cells is largely regulated by reshaping the cytoskeleton. The regulation and organization of the cytockeleton in glioma cells differs strongly from that of the normal glia cells (Hohmann and Dehghani, 2019). Compared with normal glia cells, several actin skeleton associated proteins and signaling molecules high expressed in glioma cells, such as Arp2/3, Rac1, RhoG, FAK, etc. Increased Cdc42 and Rac1 activity was observed in invading glioma cells (Hohmann and Dehghani, 2019). Besides, invading glioma cells also exhibit increased expression of FAK (Zagzag et al., 2000). Kwiatkowska et al. suggest RhoG plays an important role in the invasive behavior of glioblastoma cells (Kwiatkowska et al., 2012). CD44 could interact with various GTPases (e.g. RhoA, Rac1, and Cdc42) during tumor progression (Bourguignon, 2008).

Chemokine signaling pathway

Chemokines are a group of secreted chemotactic cytokines which play a fundamental role in immune cell migration, tumor growth, tumor angiogenesis, and tumor metastasis (Chow and Luster, 2014). Chemokines have been considered as the central components of cancer-related inflammation (Mantovani et al., 2008). The chemokine superfamily consists of about 50 chemokine ligands and 20 G protein–coupled receptors, including the CC, CXC, CX3C, and XC subfamilies (Chow and Luster, 2014). Various sets of chemokine and its corresponding chemokine receptor, including CX3CL1/CX3CR1, CXCL12/CXCR4, and CXCL16/CXCR6, contribute to tumor proliferation, migration, and invasion (Ehtesham et al., 2006; Sciume et al., 2010; Zhang et al., 2005). Further, accumulating evidence indicates that CXCL12/CXCR4 axis plays an important role in glioma cell invasion (Ehtesham et al., 2006; Zhang et al., 2005). Tang et al. suggest that CXCL12/CXCR4 expression is associated with glioma recurrence (Tang et al., 2015). Thus, chemokine signaling might have an important effect on regulation of glioma cell functions and immune cell infiltration in CD44 high

expression gliomas.

TLR signaling pathway, regulation of actin cytoskeleton, and chemokine signaling pathway are closely related with cell adhesion molecules, focal adhesion, and tumor microenvironment. The results of GSEA suggested that the poor prognosis of *CD44* high phenotype might be due, at least in part, to the distinct functions of adhesion molecules and the distinct components of the tumor microenvironment.

Conclusions

Study on key molecules in 5-ALA mediated fuorescence-guided surgery in grade II/III gliomas.

Firstly, we analyzed the correlation between clinicalpathology and fluorescence status of the grade II/III gliomas. The fluorescence status was significantly influenced by histological malignancy of gliomas. Grade II/III gliomas with IDH mutations were predominantly fluorescence-negative, whereas gliomas without IDH mutations were predominantly fluorescence-positive. Further, the MRI non-enhanced tuomors were predominantly fluorescence-negative.

Next, we found that the mRNA and protein expression levels of PEPT2 were significantly higher in the fluorescence-positive grade II/III gliomas than the fluorescence-negative grade II/III gliomas. The mRNA and protein expression levels of PEPT2 were effectively down-regulated by using siRNA.

Lastly, we found that downregulation of PEPT2 led to decreased 5-ALA mediated PpIX fluorescence intensity in human grade III glioma cell line.

In the future study, we will try to down-regulate the expression of PEPT2 in rat glioma cell line F98 and then establish the rat brain glioma model. By administrating a proper amount of 5-ALA orally to rat, we intend to try to examine the PpIX fluorescence of the glioma in the brain of the rat to further confirm the significance of PEPT2.

The present study is the first, to the best of our knowledge, to demonstrate that PEPT2 is an important gene/protein in 5-ALA-mediated FGS in lower-grade glioma. The overexpression of PEPT2 was associated with a higher fluorescence intensity of PpIX in grade II/III gliomas. These results may provide clues to improve the surgical treatment of grade II/III gliomas in the future.

Studies on the prognostic significance of CD44 in grade II/III gliomas.

Firstly, we found that *CD44* has significantly high expression in glioma tissues as compared with normal tissues. Compared with mRNA expression level of CD44s, the mRNA expression levels of *CD44v3*, *CD44v4*, *CD44v5*, *CD44v6*, *CD44v7*, *CD44v8*, *CD44v9*, and *CD44v10* were much lower. Besides, the present study suggests tumor specimens which belonged to *CD44* high group also belonged to *CD44s* high group. Thus, in grade II/III gliomas, the mRNA expression level of *CD44s* could practically represent the mRNA expression level of total *CD44*.

Then, we explored the clinical relevance of *CD44* mRNA expression based on the HUH cohorts, the TCGA cohorts, and the CGGA cohorts. In survival analysis, high mRNA expression of *CD44* was correlated with poor overall survival and poor progression-free survival in grade II/III glioma patients. Multivariate Cox regression analyses confirmed *CD44* as an independent prognostic factor for grade II/III glioma patients. According to GSEA, gene sets of Toll-like receptors (TLRs) signaling pathway, cell adhesion molecules, regulation of actin cytoskeleton, and chemokine signaling pathway are differentially enriched in *CD44* high expression phenotype.

In the future, we plan to try to down-regulate the mRNA and protein expression of CD44 in glioma cell lines and then explore the differences of proliferation, cell cycle, invasiveness between groups. If possible, *in-vivo* studies will be established to further confirm the exact function of CD44. Further, we will also focus on the mechanisms underlying the exact function of CD44. According to the results of GSEA, TLR signaling pathway, regulation of actin cytoskeleton, and chemokine pathway are related with CD44 expression. Thus, it will be of great importance for us to investigate in the genes in these pathways in the future study, such as TLR2, TLR4, TLR9, CC, and CXC family.

In conclusion, the present study demonstrated that overexpression of *CD44* is correlated with a poor prognosis for grade II/III glioma patients. Our findings suggest that *CD44* could play an important role as a useful prognostic biomarker for grade II/III glioma patients.

Acknowledgement

The study on key molecules in 5-ALA mediated fuorescence-guided surgery in grade II/III gliomas was supported by Grant-in-Aid for Young Scientists (B) (KAKENHI; grant no. 16K19991).

Disclosure of Conflict of Interest

The authors declare no conflict of interest.

References

Aldave, G., Tejada, S., Pay, E., Marigil, M., Bejarano, B., Idoate, M.A., and Diez-Valle, R. (2013). Prognostic value of residual fluorescent tissue in glioblastoma patients after gross total resection in 5-aminolevulinic Acid-guided surgery. Neurosurgery *72*, 915-920; discussion 920-911.

Anido, J., Saez-Borderias, A., Gonzalez-Junca, A., Rodon, L., Folch, G., Carmona, M.A., Prieto-Sanchez, R.M., Barba, I., Martinez-Saez, E., Prudkin, L., *et al.* (2010). TGF-beta Receptor Inhibitors Target the CD44(high)/Id1(high) Glioma-Initiating Cell Population in Human Glioblastoma. Cancer cell *18*, 655-668.

Ariza, A., Lopez, D., Mate, J.L., Isamat, M., Musulen, E., Pujol, M., Ley, A., and Navas-Palacios, J.J. (1995). Role of CD44 in the invasiveness of glioblastoma multiforme and the noninvasiveness of meningioma: an immunohistochemistry study. Human pathology *26*, 1144-1147.

Auffinger, B., Spencer, D., Pytel, P., Ahmed, A.U., and Lesniak, M.S. (2015). The role of glioma stem cells in chemotherapy resistance and glioblastoma multiforme recurrence. Expert review of neurotherapeutics *15*, 741-752.

Aydin, H., Sillenberg, I., and von Lieven, H. (2001). Patterns of failure following CT-based 3-D irradiation for malignant glioma. Strahlentherapie und Onkologie : Organ der Deutschen Rontgengesellschaft [et al] *177*, 424-431.

Bhat, K.P.L., Balasubramaniyan, V., Vaillant, B., Ezhilarasan, R., Hummelink, K., Hollingsworth, F., Wani, K., Heathcock, L., James, J.D., Goodman, L.D., *et al.* (2013). Mesenchymal differentiation mediated by NF-kappaB promotes radiation resistance in glioblastoma. Cancer cell *24*, 331-346.

Bourguignon, L.Y. (2008). Hyaluronan-mediated CD44 activation of RhoGTPase signaling and cytoskeleton function promotes tumor progression. Seminars in cancer biology *18*, 251-259.

Brown, D.V., Daniel, P.M., D'Abaco, G.M., Gogos, A., Ng, W., Morokoff, A.P., and Mantamadiotis, T. (2015). Coexpression analysis of CD133 and CD44 identifies proneural and mesenchymal subtypes of glioblastoma multiforme. Oncotarget *6*, 6267-6280.

Brown, D.V., Filiz, G., Daniel, P.M., Hollande, F., Dworkin, S., Amiridis, S., Kountouri, N., Ng, W., Morokoff, A.P., and Mantamadiotis, T. (2017). Expression of CD133 and CD44 in glioblastoma stem cells correlates with cell proliferation, phenotype stability and intra-tumor heterogeneity. PloS one *12*, e0172791.

Chen, C., Zhao, S., Karnad, A., and Freeman, J.W. (2018). The biology and role of CD44 in

cancer progression: therapeutic implications. Journal of hematology & oncology *11*, 64.

Chen, X., Keep, R.F., Liang, Y., Zhu, H.J., Hammarlund-Udenaes, M., Hu, Y., and Smith, D.E. (2017). Influence of peptide transporter 2 (PEPT2) on the distribution of cefadroxil in mouse brain: A microdialysis study. Biochemical pharmacology *131*, 89-97.

Chow, M.T., and Luster, A.D. (2014). Chemokines in cancer. Cancer immunology research *2*, 1125-1131.

Clarke, J., Butowski, N., and Chang, S. (2010). Recent advances in therapy for glioblastoma. Archives of neurology *67*, 279-283.

Dajon, M., Iribarren, K., and Cremer, I. (2017). Toll-like receptor stimulation in cancer: A pro- and anti-tumor double-edged sword. Immunobiology *222*, 89-100.

Daniel, H., and Kottra, G. (2004). The proton oligopeptide cotransporter family SLC15 in physiology and pharmacology. Pflugers Archiv : European journal of physiology *447*, 610-618.

Doring, F., Walter, J., Will, J., Focking, M., Boll, M., Amasheh, S., Clauss, W., and Daniel, H. (1998). Delta-aminolevulinic acid transport by intestinal and renal peptide transporters and its physiological and clinical implications. The Journal of clinical investigation *101*, 2761-2767.

Dosio, F., Arpicco, S., Stella, B., and Fattal, E. (2016). Hyaluronic acid for anticancer drug and nucleic acid delivery. Advanced drug delivery reviews *97*, 204-236.

Ehtesham, M., Winston, J.A., Kabos, P., and Thompson, R.C. (2006). CXCR4 expression mediates glioma cell invasiveness. Oncogene *25*, 2801-2806.

Frey, I.M., Rubio-Aliaga, I., Klempt, M., Wolf, E., and Daniel, H. (2006). Phenotype analysis of mice deficient in the peptide transporter PEPT2 in response to alterations in dietary protein intake. Pflugers Archiv : European journal of physiology *452*, 300-306.

Galli, R., Binda, E., Orfanelli, U., Cipelletti, B., Gritti, A., De Vitis, S., Fiocco, R., Foroni, C., Dimeco, F., and Vescovi, A. (2004). Isolation and characterization of tumorigenic, stem-like neural precursors from human glioblastoma. Cancer Res *64*, 7011-7021.

Groneberg, D.A., Nickolaus, M., Springer, J., Doring, F., Daniel, H., and Fischer, A. (2001). Localization of the peptide transporter PEPT2 in the lung: implications for pulmonary oligopeptide uptake. The American journal of pathology *158*, 707-714.

Gukasyan, H.J., Uchiyama, T., Kim, K.J., Ehrhardt, C., Wu, S.K., Borok, Z., Crandall, E.D., and Lee, V.H.L. (2017). Oligopeptide Transport in Rat Lung Alveolar Epithelial Cells is

Mediated by Pept2. Pharmaceutical research *34*, 2488-2497.

Hohmann, T., and Dehghani, F. (2019). The Cytoskeleton-A Complex Interacting Meshwork. Cells *8*.

Hu, Y., Ocheltree, S.M., Xiang, J., Keep, R.F., and Smith, D.E. (2005). Glycyl-L-glutamine disposition in rat choroid plexus epithelial cells in primary culture: role of PEPT2. Pharmaceutical research *22*, 1281-1286.

Hu, Y., Shen, H., Keep, R.F., and Smith, D.E. (2007). Peptide transporter 2 (PEPT2) expression in brain protects against 5-aminolevulinic acid neurotoxicity. Journal of neurochemistry *103*, 2058-2065.

Jaber, M., Wolfer, J., Ewelt, C., Holling, M., Hasselblatt, M., Niederstadt, T., Zoubi, T., Weckesser, M., and Stummer, W. (2016). The Value of 5-Aminolevulinic Acid in Low-grade Gliomas and High-grade Gliomas Lacking Glioblastoma Imaging Features: An Analysis Based on Fluorescence, Magnetic Resonance Imaging, 18F-Fluoroethyl Tyrosine Positron Emission Tomography, and Tumor Molecular Factors. Neurosurgery *78*, 401-411; discussion 411.

Jiang, Y., Zhou, J., Luo, P., Gao, H., Ma, Y., Chen, Y.S., Li, L., Zou, D., Zhang, Y., and Jing, Z. (2018). Prosaposin promotes the proliferation and tumorigenesis of glioma through toll-like receptor 4 (TLR4)-mediated NF-kappaB signaling pathway. EBioMedicine *37*, 78-90.

Jijiwa, M., Demir, H., Gupta, S., Leung, C., Joshi, K., Orozco, N., Huang, T., Yildiz, V.O., Shibahara, I., de Jesus, J.A., *et al.* (2011). CD44v6 regulates growth of brain tumor stem cells partially through the AKT-mediated pathway. PloS one *6*, e24217.

Kaaijk, P., Troost, D., Morsink, F., Keehnen, R.M., Leenstra, S., Bosch, D.A., and Pals, S.T. (1995). Expression of CD44 splice variants in human primary brain tumors. J Neurooncol *26*, 185-190.

Klank, R.L., Decker Grunke, S.A., Bangasser, B.L., Forster, C.L., Price, M.A., Odde, T.J., SantaCruz, K.S., Rosenfeld, S.S., Canoll, P., Turley, E.A., *et al.* (2017). Biphasic Dependence of Glioma Survival and Cell Migration on CD44 Expression Level. Cell reports *18*, 23-31.

Kwiatkowska, A., Didier, S., Fortin, S., Chuang, Y., White, T., Berens, M.E., Rushing, E., Eschbacher, J., Tran, N.L., Chan, A., *et al.* (2012). The small GTPase RhoG mediates glioblastoma cell invasion. Molecular cancer *11*, 65.

Lacroix, M., Abi-Said, D., Fourney, D.R., Gokaslan, Z.L., Shi, W., DeMonte, F., Lang, F.F., McCutcheon, I.E., Hassenbusch, S.J., Holland, E., *et al.* (2001). A multivariate analysis of

416 patients with glioblastoma multiforme: prognosis, extent of resection, and survival. Journal of neurosurgery *95*, 190-198.

Li, C., Ma, L., Liu, Y., Li, Z., Wang, Q., Chen, Z., Geng, X., Han, X., Sun, J., and Li, Z. (2019). TLR2 promotes development and progression of human glioma via enhancing autophagy. Gene *700*, 52-59.

Li, H., Hamou, M.F., de Tribolet, N., Jaufeerally, R., Hofmann, M., Diserens, A.C., and Van Meir, E.G. (1993). Variant CD44 adhesion molecules are expressed in human brain metastases but not in glioblastomas. Cancer Res *53*, 5345-5349.

Li, H., Liu, J., and Hofmann, M. (1995). [CD44 expression patterns in primary and secondary brain tumors]. Zhonghua yi xue za zhi *75*, 525-528, 573.

Liu, W., Liang, R., Ramamoorthy, S., Fei, Y.J., Ganapathy, M.E., Hediger, M.A., Ganapathy, V., and Leibach, F.H. (1995). Molecular cloning of PEPT 2, a new member of the H+/peptide cotransporter family, from human kidney. Biochimica et biophysica acta *1235*, 461-466.

Livak, K.J., and Schmittgen, T.D. (2001). Analysis of relative gene expression data using real-time quantitative PCR and the 2(-Delta Delta C(T)) Method. Methods *25*, 402-408.

Mantovani, A., Allavena, P., Sica, A., and Balkwill, F. (2008). Cancer-related inflammation. Nature *454*, 436-444.

Miwa, T., Nagata, T., Kojima, H., Sekine, S., and Okumura, T. (2017). Isoform switch of CD44 induces different chemotactic and tumorigenic ability in gallbladder cancer. International journal of oncology *51*, 771-780.

Nishikawa, M., Inoue, A., Ohnishi, T., Kohno, S., Ohue, S., Matsumoto, S., Suehiro, S., Yamashita, D., Ozaki, S., Watanabe, H., *et al.* (2018). Significance of Glioma Stem-Like Cells in the Tumor Periphery That Express High Levels of CD44 in Tumor Invasion, Early Progression, and Poor Prognosis in Glioblastoma. Stem cells international *2018*, 5387041.

Novotny, A., Xiang, J., Stummer, W., Teuscher, N.S., Smith, D.E., and Keep, R.F. (2000). Mechanisms of 5-aminolevulinic acid uptake at the choroid plexus. Journal of neurochemistry *75*, 321-328.

Ostrom, Q.T., Gittleman, H., Truitt, G., Boscia, A., Kruchko, C., and Barnholtz-Sloan, J.S. (2018). CBTRUS Statistical Report: Primary Brain and Other Central Nervous System Tumors Diagnosed in the United States in 2011-2015. Neuro-oncology *20*, iv1-iv86.

Pietras, A., Katz, A.M., Ekstrom, E.J., Wee, B., Halliday, J.J., Pitter, K.L., Werbeck, J.L., Amankulor, N.M., Huse, J.T., and Holland, E.C. (2014). Osteopontin-CD44 signaling in the glioma perivascular niche enhances cancer stem cell phenotypes and promotes aggressive

tumor growth. Cell stem cell *14*, 357-369.

Ponta, H., Sherman, L., and Herrlich, P.A. (2003). CD44: from adhesion molecules to signalling regulators. Nature reviews Molecular cell biology *4*, 33-45.

Prochazka, L., Tesarik, R., and Turanek, J. (2014). Regulation of alternative splicing of CD44 in cancer. Cellular signalling *26*, 2234-2239.

Qadri, M., Almadani, S., Jay, G.D., and Elsaid, K.A. (2018). Role of CD44 in Regulating TLR2 Activation of Human Macrophages and Downstream Expression of Proinflammatory Cytokines. J Immunol *200*, 758-767.

Ranuncolo, S.M., Ladeda, V., Specterman, S., Varela, M., Lastiri, J., Morandi, A., Matos, E., Bal de Kier Joffe, E., Puricelli, L., and Pallotta, M.G. (2002). CD44 expression in human gliomas. Journal of surgical oncology *79*, 30-35; discussion 35-36.

Resnick, D.K., Resnick, N.M., Welch, W.C., and Cooper, D.L. (1999). Differential expressions of CD44 variants in tumors affecting the central nervous system. Molecular diagnosis : a journal devoted to the understanding of human disease through the clinical application of molecular biology *4*, 219-232.

Rubio-Aliaga, I., and Daniel, H. (2002). Mammalian peptide transporters as targets for drug delivery. Trends in pharmacological sciences *23*, 434-440.

Rubio-Aliaga, I., Frey, I., Boll, M., Groneberg, D.A., Eichinger, H.M., Balling, R., and Daniel, H. (2003). Targeted disruption of the peptide transporter Pept2 gene in mice defines its physiological role in the kidney. Molecular and cellular biology *23*, 3247-3252.

Sala-Rabanal, M., Loo, D.D., Hirayama, B.A., and Wright, E.M. (2008). Molecular mechanism of dipeptide and drug transport by the human renal H+/oligopeptide cotransporter hPEPT2. American journal of physiology Renal physiology *294*, F1422-1432.

Sanai, N., and Berger, M.S. (2008). Glioma extent of resection and its impact on patient outcome. Neurosurgery *62*, 753-764; discussion 264-756.

Sciume, G., Soriani, A., Piccoli, M., Frati, L., Santoni, A., and Bernardini, G. (2010). CX3CR1/CX3CL1 axis negatively controls glioma cell invasion and is modulated by transforming growth factor-beta1. Neuro-oncology *12*, 701-710.

Shen, H., Ocheltree, S.M., Hu, Y., Keep, R.F., and Smith, D.E. (2007). Impact of genetic knockout of PEPT2 on cefadroxil pharmacokinetics, renal tubular reabsorption, and brain penetration in mice. Drug metabolism and disposition: the biological fate of chemicals *35*, 1209-1216.

Singh, S.K., Hawkins, C., Clarke, I.D., Squire, J.A., Bayani, J., Hide, T., Henkelman, R.M., Cusimano, M.D., and Dirks, P.B. (2004). Identification of human brain tumour initiating cells. Nature *432*, 396-401.

Stummer, W., Pichlmeier, U., Meinel, T., Wiestler, O.D., Zanella, F., Reulen, H.J., and Group, A.L.-G.S. (2006). Fluorescence-guided surgery with 5-aminolevulinic acid for resection of malignant glioma: a randomised controlled multicentre phase III trial. The Lancet Oncology *7*, 392-401.

Stummer, W., Stocker, S., Wagner, S., Stepp, H., Fritsch, C., Goetz, C., Goetz, A.E., Kiefmann, R., and Reulen, H.J. (1998). Intraoperative detection of malignant gliomas by 5-aminolevulinic acid-induced porphyrin fluorescence. Neurosurgery *42*, 518-525; discussion 525-516.

Stupp, R., Mason, W.P., van den Bent, M.J., Weller, M., Fisher, B., Taphoorn, M.J., Belanger, K., Brandes, A.A., Marosi, C., Bogdahn, U., *et al.* (2005). Radiotherapy plus concomitant and adjuvant temozolomide for glioblastoma. The New England journal of medicine *352*, 987-996.

Svitkina, T.M. (2018). Ultrastructure of the actin cytoskeleton. Current opinion in cell biology *54*, 1-8.

Takahashi, K., Ikeda, N., Nonoguchi, N., Kajimoto, Y., Miyatake, S., Hagiya, Y., Ogura, S., Nakagawa, H., Ishikawa, T., and Kuroiwa, T. (2011). Enhanced expression of coproporphyrinogen oxidase in malignant brain tumors: CPOX expression and 5-ALA-induced fluorescence. Neuro-oncology *13*, 1234-1243.

Tammi, R.H., Kultti, A., Kosma, V.M., Pirinen, R., Auvinen, P., and Tammi, M.I. (2008). Hyaluronan in human tumors: pathobiological and prognostic messages from cell-associated and stromal hyaluronan. Seminars in cancer biology *18*, 288-295.

Tanaka, S., Nakada, M., Yamada, D., Nakano, I., Todo, T., Ino, Y., Hoshii, T., Tadokoro, Y., Ohta, K., Ali, M.A., *et al.* (2015). Strong therapeutic potential of gamma-secretase inhibitor MRK003 for CD44-high and CD133-low glioblastoma initiating cells. J Neurooncol *121*, 239-250.

Tang, W., Wang, X., Chen, Y., Zhang, J., Chen, Y., and Lin, Z. (2015). CXCL12 and CXCR4 as predictive biomarkers of glioma recurrence pattern after total resection. Pathologie-biologie *63*, 190-198.

Terada, T., and Inui, K. (2004). Peptide transporters: structure, function, regulation and application for drug delivery. Current drug metabolism *5*, 85-94.

Terada, T., Saito, H., Sawada, K., Hashimoto, Y., and Inui, K. (2000). N-terminal halves of

rat H+/peptide transporters are responsible for their substrate recognition. Pharmaceutical research *17*, 15-20.

Theeler, B.J., and Groves, M.D. (2011). High-grade gliomas. Current treatment options in neurology *13*, 386-399.

Toole, B.P. (2004). Hyaluronan: from extracellular glue to pericellular cue. Nature reviews Cancer *4*, 528-539.

Tsidulko, A.Y., Kazanskaya, G.M., Kostromskaya, D.V., Aidagulova, S.V., Kiselev, R.S., Volkov, A.M., Kobozev, V.V., Gaitan, A.S., Krivoshapkin, A.L., and Grigorieva, E.V. (2017). Prognostic relevance of NG2/CSPG4, CD44 and Ki-67 in patients with glioblastoma. Tumour biology : the journal of the International Society for Oncodevelopmental Biology and Medicine *39*, 1010428317724282.

Utsuki, S., Oka, H., Sato, S., Suzuki, S., Shimizu, S., Tanaka, S., and Fujii, K. (2006). Possibility of using laser spectroscopy for the intraoperative detection of nonfluorescing brain tumors and the boundaries of brain tumor infiltrates. Technical note. Journal of neurosurgery *104*, 618-620.

Verrey, F., Singer, D., Ramadan, T., Vuille-dit-Bille, R.N., Mariotta, L., and Camargo, S.M. (2009). Kidney amino acid transport. Pflugers Archiv : European journal of physiology *458*, 53-60.

Wallner, K.E., Galicich, J.H., Krol, G., Arbit, E., and Malkin, M.G. (1989). Patterns of failure following treatment for glioblastoma multiforme and anaplastic astrocytoma. International journal of radiation oncology, biology, physics *16*, 1405-1409.

Wang, C., Cao, S., Yan, Y., Ying, Q., Jiang, T., Xu, K., and Wu, A. (2010). TLR9 expression in glioma tissues correlated to glioma progression and the prognosis of GBM patients. BMC cancer *10*, 415.

Wang, F., Zheng, Z., Guan, J., Qi, D., Zhou, S., Shen, X., Wang, F., Wenkert, D., Kirmani, B., Solouki, T., *et al.* (2018). Identification of a panel of genes as a prognostic biomarker for glioblastoma. EBioMedicine *37*, 68-77.

Wang, H.H., Liao, C.C., Chow, N.H., Huang, L.L., Chuang, J.I., Wei, K.C., and Shin, J.W. (2017). Whether CD44 is an applicable marker for glioma stem cells. American journal of translational research *9*, 4785-4806.

Wang, M., Zhang, X., Zhao, H., Wang, Q., and Pan, Y. (2010). Comparative analysis of vertebrate PEPT1 and PEPT2 genes. Genetica *138*, 587-599.

Wei, K.C., Huang, C.Y., Chen, P.Y., Feng, L.Y., Wu, T.W., Chen, S.M., Tsai, H.C., Lu, Y.J.,

Tsang, N.M., Tseng, C.K., *et al.* (2010). Evaluation of the prognostic value of CD44 in glioblastoma multiforme. Anticancer research *30*, 253-259.

Yan, Y., Zuo, X., and Wei, D. (2015). Concise Review: Emerging Role of CD44 in Cancer Stem Cells: A Promising Biomarker and Therapeutic Target. Stem cells translational medicine *4*, 1033-1043.

Ylagan, L.R., and Quinn, B. (1997). CD44 expression in astrocytic tumors. Modern pathology : an official journal of the United States and Canadian Academy of Pathology, Inc *10*, 1239-1246.

Zagzag, D., Friedlander, D.R., Margolis, B., Grumet, M., Semenza, G.L., Zhong, H., Simons, J.W., Holash, J., Wiegand, S.J., and Yancopoulos, G.D. (2000). Molecular events implicated in brain tumor angiogenesis and invasion. Pediatric neurosurgery *33*, 49-55.

Zhang, J., Sarkar, S., and Yong, V.W. (2005). The chemokine stromal cell derived factor-1 (CXCL12) promotes glioma invasiveness through MT2-matrix metalloproteinase. Carcinogenesis *26*, 2069-2077.

Zhao, S.G., Chen, X.F., Wang, L.G., Yang, G., Han, D.Y., Teng, L., Yang, M.C., Wang, D.Y., Shi, C., Liu, Y.H., *et al.* (2013). Increased expression of ABCB6 enhances protoporphyrin IX accumulation and photodynamic effect in human glioma. Annals of surgical oncology *20*, 4379-4388.